Published in final edited form as:
Neurobiol Dis. 2013 November ; 59: 1–17. doi:10.1016/j.nbd.2013.06.013.

Phosphorylation of FMRP and alterations of FMRP complex underlie enhanced mLTD in adult rats triggered by early life seizures

Paul B. Bernard[1], **Anna M. Castano**[1], **Heather O'Leary**[1], **Kameron Simpson**[3], **Michael D. Browning**[3], and **Tim. A. Benke**[1,2,4]

[1]Department of Pediatrics, University of Colorado, Aurora, CO

[2]Department of Neuroscience Graduate Program, University of Colorado, Aurora, CO

[3]School of Medicine PhosphoSolutions, University of Colorado, Aurora, CO

[4]Department of Neurology, Pharmacology, and Otolaryngology, University of Colorado, Aurora, CO

Abstract

Outside of Fragile X syndrome (FXS), the role of Fragile-X Mental Retardation Protein (FMRP) in mediating neuropsychological abnormalities is not clear. FMRP, p70-S6 kinase (S6K) and protein phosphatase 2A (PP2A) are thought to cooperate as a dynamic signaling complex. In our prior work, adult rats have enhanced CA1 hippocampal long-term depression (LTD) following an early life seizure (ELS). We now show that mGluR-mediated LTD (mLTD) is specifically enhanced following ELS, similar to FMRP knock-outs. Total FMRP expression is unchanged but S6K is hyperphosphorylated, consistent with S6K overactivation. We postulated that either disruption of the FMRP-S6K-PP2A complex and/or removal of this complex from synapses could explain our findings. Using subcellular fractionation, we were surprised to find that concentrations of FMRP and PP2A were undisturbed in the synaptosomal compartment but reduced in parallel in the cytosolic compartment. Following ELS FMRP phosphorylation was reduced in the cytosolic compartment and increased in the synaptic compartment, in parallel with the compartmentalization of S6K activation. Furthermore, FMRP and PP2A remain bound following ELS. In contrast, the interaction of S6K with FMRP is reduced by ELS. Blockade of PP2A results in enhanced mLTD; this is occluded by ELS. This suggests a critical role for the location and function of the FMRP-S6K-PP2A signaling complex in limiting the amount of mLTD. Specifically, non-synaptic targeting and the function of the complex may influence the "set-point" for regulating mLTD. Consistent with this, striatal-enriched protein tyrosine phosphatase (STEP), an FMRP "target" which regulates mLTD expression, is specifically increased in the synaptosomal compartment following ELS. Further, we provide behavioral data to suggest that

Corresponding author: Tim A. Benke, University of Colorado Denver, School of Medicine, 12800 E 19th, MS8102, Denver, CO 80045, tim.benke@ucdenver.edu; 303 724-3568; 303 724 2439.

Author responsibilities

PBB, AMC and TAB designed, performed and analyzed the experiments. KS and MDB generated and assisted in the characterization of the 6058 antibody. HC characterized 6058 interactions with FMRP mutants. PBB and TAB co-wrote the paper, all proof-read the paper; TAB supervised the project. MDB and KS have a financial interest in 6058. The authors otherwise declare no conflicts of interest.

FMRP complex dysfunction may underlie altered socialization, a symptom associated and observed in other rodent models of autism, including FXS.

Keywords

Seizure; Long-term depression (LTD); Metabotropic glutamate receptor (mGluR); Fragile X Mental Retardation Protein (FMRP); Protein phosphatase 2A (PP2A); Striatal-enriched tyrosine protein phosphatase (STEP)

Introduction

Early life seizures (ELS) have been independently associated with adverse developmental outcomes that include intellectual disability (ID) and autism (McBride et al., 2000;Ortibus et al., 1996;Miller et al., 2002;Saemundsen et al., 2007). While possibly a proxy for other brain injuries, the odds-ratio of autism is 3-fold higher in pre-term infants with seizures (Buchmayer et al., 2009). Despite their association, seizures and/or epilepsy are not a clearly defined cause of ID and autism (Tuchman et al., 2009). Mutations in the FMR1 gene result in loss of function of the Fragile-X Mental Retardation Protein (FMRP) and are linked to ID and autism in Fragile X Syndrome (FXS). In FXS, the presence of seizures is associated with a greater risk for autism (Hagerman et al., 2010). Outside of FXS, the role of FMRP function in mediating autism and or ID is not clear. Postmortem studies in individuals with idiopathic autism may link dysregulation of FMRP expression with seizures (Fatemi and Folsom, 2011). A genetic study of idiopathic autism has implicated FMRP-associated genes (Iossifov et al., 2012). However, the links between early-life seizures, idiopathic ID/autism and FMRP remain circumstantial.

In adult rodents, long-term depression (LTD) is primarily induced through activation of mGluRs (Gladding et al., 2009;Luscher and Huber, 2010). Synaptically localized (Stefani et al., 2004) and phosphorylated FMRP acts as a negative regulator of translation under basal conditions (Narayanan et al., 2007;Bassell and Warren, 2008). In current schema, mGluR-mediated signaling first leads to activation of PP2A and dephosphorylation of FMRP (activating translation) while further mGluR-mediated activation (via AKT) secondarily leads to re-phosphorylation of FMRP via p70-S6 kinase (S6K) (stalling translation) (Ceman et al., 2003;Narayanan et al., 2007;Bassell and Warren, 2008;Narayanan et al., 2008). Hyperactivation of S6K via AKT is suggested in loss of FMRP (Sharma et al., 2010) (but see (Hu et al., 2008)). FMRP activity may be further mediated by the dynamic binding interactions of FMRP, PP2A and S6K (Narayanan et al., 2008). Blockade of PP2A and/or protein phosphatase 1 (PP1) results in exaggerated mLTD (Schnabel et al., 2001). However, a recent report suggests PP2A blockade transiently reduces mLTD (Niere et al., 2012). mLTD induction is critically dependent on protein synthesis (Huber et al., 2000). mLTD becomes protein synthesis independent or saturated (Osterweil et al., 2010) with complete genetic loss of FMRP resulting in enhanced mLTD (Nosyreva and Huber, 2006;Volk et al., 2007)). However, with only modest reductions of FMRP expression, mLTD remains enhanced and dependent on protein synthesis{20459}. Synthesis of striatal enriched protein tyrosine phosphatase (STEP) is controlled by FMRP (Darnell et al., 2011); synthesis and activation of STEP leads to dephosphorylation of synaptic AMPAR that triggers their removal to mediate mLTD expression (Moult et al., 2006;Zhang et al., 2008).

Previously we reported non-specific enhancement of LTD in adult rats following ELS, without changes in hippocampal cytoarchitecture or baseline synaptic functions (Cornejo et al., 2007). We now show that the enhanced LTD following ELS is specific for mLTD. We demonstrate that the FMRP-S6K-PP2A signaling complex is disrupted by ELS. Blockade of

PP2A results in enhanced mLTD; this is occluded by ELS. Further, STEP expression is enhanced post-synaptically by ELS, altering the "set point" for mLTD expression. Previously we reported alterations in working memory (Cornejo et al., 2007;Cornejo et al., 2008) and exaggerated fear conditioned responses (Cornejo et al., 2008). We now show abnormal social interaction, a symptom associated with autism. Thus, we link ELS with FMRP dysfunction that may underlie other mechanisms of ID with autism features outside of genetic loss of FMRP in FXS.

Materials and Methods

Animals

All studies conformed to the requirements of the National Institutes of Health *Guide for the Care and Use of Laboratory Animals* and were approved by the Institutional Animal Care and Use subcommittee of the University of Colorado Health Sciences Center. Timed-pregnant Sprague Dawley rats (Charles Rivers Labs, Wilmington, MA) gave birth in-house. Background (FVB.129P2-Pde6b<+> Tyr<c-ch>/AntJ) and FMR1KO (FVB.129P2-Pde6b<+> Tyr<c-ch> Fmr1<tm1Cgr>/J) mice were obtained from Jackson Laboratory (Bar Harbor, ME). All rodents were housed in micro-isolator cages with water and chow available *ad libitum*.

Seizure Induction

Kainic acid (KA), a fixed glutamate analog (Dingledine et al., 1999), was used to induce temporal-lobe seizures (Tremblay et al., 1984) as done in previous studies(Cornejo et al., 2007;Cornejo et al., 2008). Male rat pups were subcutaneously injected with KA (2 mg/kg; Tocris, Ellisville, MO) on P7 (P0 defined as the date of birth) resulting in discontinuous behavioral and electrical seizure activity lasting up to three hours(Dzhala et al., 2005). Mortality was less than 3%. Onset of seizure activity occurred within 30 min of injection and was characterized by intermittent myoclonic jerks, generalized tonic-clonic jerks, scratching, "swimming", and "wet-dog shakes." Control male rat pups were injected with an equivalent volume of 0.9% saline. Male pups were chosen in order to eliminate the effects of hormonal cycles on behavior. Rats were then tagged with a microchip (Avid Identification Systems, Norco, CA) so that experimenters remained blinded to the treatment. Offspring were returned to their dam after observable seizure activity ceased. Rats were weaned and separated according to gender at P20–22. At P60–80 (unless otherwise indicated), video-EEG, behavioral, immunocytochemical, electrophysiological and biochemical analyses were undertaken with male rats.

Video-EEG monitoring

As described previously(Raol et al., 2006), P60–80 male rats were anesthetized with ketamine (100 mg/kg) and xylaxine (15 mg/kg), followed by continuous isoflurane (1–4%) and placed in a stereotaxic frame (David Kopf Instruments, Tujunga, CA). Four saline injected controls and 6 ELS rats were implanted with an electrode in frontal cortex (from bregma, AP 2.0 mm, ML 3 mm) and bilateral CA1 of hippocampi (from bregma, AP −3.3 mm, ML 2.0 mm, DV 2.6 mm) for combined intracranial electroencephalography (EEG) and video monitoring (Pinnacle Systems, Lawrence, KS). After 1 week recovery, rats were monitored continuously, 24h/d, for 5–17 days.

Hippocampal Slice Preparation and Electrophysiology

As done previously(Cornejo et al., 2007), following rapid decapitation and removal of the brain, sagittal hippocampal slices (400 μm) were made using a vibratome (Vibratome, St Louis, MO) in ice-cold sucrose artificial cerebral spinal fluid (sACSF: 206 mM sucrose, 2.8

mM KCl, 1 mM $CaCl_2$, 3 mM $MgSO_4$, 1.25 mM NaH_2PO_4, 26 mM $NaHCO_3$, 10 mM D-glucose and bubbled with 95%/5% O_2/CO_2) (Kuenzi et al., 2000). Following removal of CA3, slices were recovered in a submersion type chamber perfused with oxygenated artificial cerebral spinal fluid (ACSF: 124 mM NaCl, 3 mM KCl, 1 mM $MgSO_4$, 2 mM $CaCl_2$, 1.2 mM NaH_2PO_4, 26 mM NaHCO3, 10 mM D-glucose and bubbled with 95%/5% O_2/CO_2) at 28°C for at least 90 min and then submerged in a recording chamber perfused with ACSF. All electrophysiology was performed in the CA1 region at 28°C. Two twisted-tungsten bipolar stimulating electrodes were offset in the CA1 to stimulate two independent Schaffer collateral-commissural pathways using a constant current source (WPI, Sarasota, FL) with a fixed duration (20 μs), each at a rate of 0.033 Hz. Field excitatory post-synaptic potentials (fEPSPs) were recorded from the stratum radiatum region of CA1 using a borosilicate glass (WPI, Sarasota, Fl) microelectrode (pulled (Sutter, Novato, CA) to 6 to 9 MΩ when filled with 3M NaCl), amplified 1000× (WPI, Sarasota, Fl and Warner, Hamden, CT), and digitized (National Instruments, Austin, Texas) at 10 kHz using winLTP-version 2.4(Anderson and Collingridge, 2001) to follow fEPSP slope (averaged over 4 EPSPs), measured using 20% to 80% rise times, expressed as percent of baseline, during the course of an experiment. In order to be sure only “healthy” slices were included in our studies, responses had to meet several criteria: fiber volleys less than 1/3 of response amplitude and peak responses larger than 0.6 mV; responses and fiber volley must be stable (<5% drift). In the presence of D-APV (50 μM, Tocris, Ellisville, MO) and following baseline stabilization of fEPSP slope at approximately 75% of maximal slope for at least 30 min, mLTD was induced in one pathway (900 paired-pulse stimuli at 1 Hz with 50 ms inter-pulse interval, SPP-LFS). In some experiments, chemical mLTD was induced (DHPG × 100 μM × 10 mins) 60 minutes later to both pathways (naïve and prior electrical LTD). Dead volume was kept to a minimum (9–10 mL) and flow rate was always tightly controlled (2–3 mL/min). D-APV was omitted only in the experiment to minimize mLTD; LTD was induced with 900 paired-pulse stimuli at 1 Hz with 200 ms inter-pulse interval (LPP-LFS)(Kemp et al., 2000). It has been demonstrated in rats that using 50 ms inter-pulse interval facilitates mLTD, while a 200 ms interval favors NMDAR mediated LTD (Kemp et al., 2000). Where indicated, slices were incubated in anisomycin (20 μM for one hour prior to and during recording, Tocris, Ellisville, MO), cycloheximide (60 μM for 30 min prior to and during recording, Tocris, Ellisville, MO) or okadaic acid (3 nM for 30 min prior to and during recording, Tocris, Ellisville, MO).

Western blotting

Hippocampal slices were prepared and recovered as for electrophysiology with the addition of cuts to isolate CA1 from the remaining hippocampus; after recovery, the slices were suspended in STE buffer, sonicated, boiled for 5 minutes and then frozen until further use. In order to minimize the effects of slice preparation(Osterweil et al., 2010) and to control for slice quality, only slices that came from a preparation that met electrophysiological criteria were used. All concentrations were quantified with BCA and then loaded in duplicate on 10% polyacrylamide gel and a five-point dilution series of naive rat hippocampal homogenate was included on each gel as a standard curve for quantification of immunoreactivity/μg loaded protein(Grosshans and Browning, 2001). Following transfer to PolyScreen PVDF transfer membrane (Genie, Idea Scientific Company, Minneapolis, MN, USA), blots were blocked in BSA or Carnation nonfat dry milk for 1 h and incubated either 1h at room temperature or overnight at 4°C with antibodies (Table 1). Blots were then subjected to three 10-min washings in Tris-buffered saline (140 mm NaCl, 20 mm Tris pH 7.6) plus 0.1% Tween 20 (TTBS), before being incubated with anti-mouse or anti-rabbit secondary antibody (1:5000) in 1% BSA or milk for 1 h at room temperature, followed by three additional 10-min washes preformed with TTBS. Immunodetection was accomplished using a chemiluminescent substrate kit (SuperSignal West Femto Maximum Sensitivity

Substrate; Pierce) and the Alpha Innotech (Alpha Innotech, San Leandro, CA, USA) imaging system. Quantification was performed using AlphaEase software (Alpha Innotech, San Leandro, CA, USA) and Excel (Microsoft, Redmond, WA, USA). Immunoreactivity was reported as the density of sample bands relative to the standard curve. For phospho-proteins, ratios of immunoreactivity/μg to totals are reported without standardization. Only values falling within the standard curve generated from the dilution series included on each gel were incorporated into the final analysis. Some of the blots were then stripped (Restore PLUS Western Blot Stripping Buffer; Thermo Scientific, Rockford, IL) and reblotted if needed.

Subcellular fractionation

Hippocampal slices were prepared and recovered as for electrophysiology and western blotting with the addition of cuts to isolate CA1 from the remaining hippocampus; after recovery, slices were placed in ice-cold buffered sucrose solution (50μL per slice) containing 320mM sucrose, 10mM Tris (pH 7.4), 40mM NaF, 300 nM okadaic acid, 1mM EDTA and 1mM EGTA. Slices were immediately homogenized in a glass grinding vessel by Teflon pestle rotating at 1000 RPM. Homogenates were then centrifuged at 1000×g for 10min. The pellet (P1), which contains nuclei and incompletely homogenized cells, was suspended (200μL 1× STE), sonicated and boiled for 5min at 100°C. The supernatant (S1) was centrifuged at 10,000×g for 15min. The pellet (P2), which contains synaptosomal plasma membrane, was suspended in 50 μL of 1× STE, sonicated and boiled. The supernatant (S2), which contains the soluble fraction, was precipitated with cold Acetone (4×) for at least 12h at −20°C, centrifuged at 15,000×g for 10min, air dried, suspended in 30μL of 1× STE, sonicated and boiled. Protein concentrations were quantified with BCA and then kept frozen until further semi-quantitative analysis as performed for western blotting.

Immunoprecipitation

Hippocampal slices were prepared and recovered as for electrophysiology and western blotting with the addition of cuts to isolate CA1 from the remaining hippocampus; after recovery, slices were placed in ice-cold buffer (450μL) containing 10mM HEPES pH 7.4, 200mM NaCl, 20mM NaF, 0.5% TritionX-100, 300 nM okadaic acid, 30mM EDTA and protease inhibitor cocktail (#78410, Thermo Scientific, Rockford, IL). All manipulations were performed at 4°C or on ice. The slices were immediately homogenized in a glass grinding vessel by Teflon pestle rotating at 1000 RPM. Homogenates were then centrifuged at 3000×g for 10min; the pellet was washed with 450μL of buffer and re-pelleted. Supernatants were pooled and clarified at 70,000×g for 30min. The resulting supernatant was pre-cleared for one hour with 50μl MagnaBind protein G beads (# 21349, Thermo Scientific, Rockford, IL). Protein concentrations were quantified with BCA; 500μg of total protein was then immunoprecipitated with anti-FMRP 7G1–1 mAb (Developmental Studies Hybridoma Bank) conjugated to 50ul of Protein G beads overnight at 4°C. Beads were washed 3× in binding buffer (100mM Na_2HPO_4 pH 5.5, 150mM NaCl), re-suspended in 50μl of 4× loading buffer and further semi-quantitative analysis was performed as for western blotting.

Generation and characterization of phosphorylated FMRP antibody

Phosphorylated-FMRP antibody (6058) was generated by immunization of rabbits with a peptide corresponding to amino-acids 483 to 521 of FMRP which included the primary phosphorylation site S499(Ceman et al., 2003) (PhosphoSolutions, Aurora, CO). Hippocampal slices, prepared as above, were treated with DHPG (100 μM × 30 mins) or control and then subjected to westernblot analysis. For phosphatase treatment, control slices were sonicated in lysis buffer (1% NP40, 10mM Tris/ HCl (pH 7.4), 1mM EDTA, 100mM

NaCl). 750 µl (protein concentration ~2.0 mg/ml) of each sample was then subjected to phosphatase treatment while the remaining 750 µl was brought to 1% SDS. In the phosphatase treatment, the samples were brought to a concentration of 2 mM $MnCl_2$, 1 mM EDTA, 5 mM dithiothreital and 0.01% Brij 35 by addition of a 10× concentrated solution. Samples were then incubated for 30 min (room temperature) in the presence of ~30,000 units of lambda phosphatase (# P9614, Sigma, St. Louis, MO) and ~7500 units of alkaline phosphatase (# P0114, Sigma, St. Louis, MO). The reaction was stopped by the addition of 10% SDS to yield a final concentration of 1% SDS. Western blotting was performed as above.

Cell culture, transfection, and harvesting

Human Embryonic Kidney cells (HEK293) were maintained in DMEM supplemented with 10% Fetal Bovine Serum and 50 U/ml penicillin/streptomycin (Invitrogen) at 37°C, 5% CO_2. HEK293 cells were transfected using the Calcium Phosphate method, described briefly here. One day prior to transfection confluent cells were split 1:5 onto 10cm culture dishes. Flag-tagged FMR1 wild type, mutant S499A (kindly provided by Stephen Warren, PhD, Emory University, Atlanta GA), or no DNA control (16µg DNA/10cm dish) were precipitated with 0.125M $CaCl_2$, and 1× HBS (in mM: 137 NaCl, 5 KCl, 0.7 $Na_2HPO_4{\cdot}7H_2O$, 7.5 glucose, 21 HEPES) for 30 minutes at RT shielded from light. The precipitated DNA was added to HEK293 cells. The cells were returned to the incubator for overnight incubation (~16 hrs), before culture medium was exchanged. After 72 hours, transfected HEK293 cells were washed 1× in PBS containing $CaCl_2$. The cells were then harvested on ice in IP Buffer lacking TritonX-100 (see recipe under *Immunoprecipitation*) (1ml/10cm dish). Immunoprecipitation of Flag-tagged FMR protein and Western Blotting were then performed as described (*Immunoprecipitation and Western Blotting*). Immunoprecipitation from cultured cells was performed using anti-Flag Ab (F1804).

Immunocytochemisty

Hippocampal slices (400 µm) were prepared and recovered as for electrophysiology. Slices were transferred to ice-cold ACSF, fixed with 4% paraformaldehyde in phosphate buffered saline (PBS) for 4 hours, washed 3× with PBS with 0.01% NaN_3 (PBSN) and then suspended in PBSN with 30% sucrose at 4°C for 72–96h. Slices were quickly frozen with dry ice and sliced sagitally at 40 µm with a sliding microtome and washed with PBSN × 3. Slices were blocked with PBS + 1% BSA + 2% GS + 0.3% triton (BA) at room temperature for 2h and then incubated with 1:500 mouse anti-FMRP (1C3)(Antar et al., 2004;Antar et al., 2005;Hou et al., 2006) and 1:500 rabbit anti-MAP2 (Millipore, Billerica, MA) for 48–72h at 4°C. After washing with PBSN × 3, slices were blocked in BA at 4°C for 24 h and then incubated with 1:400 goat anti-mouse Alexa Fluor 488 and 1:400 goat anti-rabbit Alexa Fluor 568 (Invitrogen, Carlsbad, CA) at 4°C for 24 h. After washing with PBSN × 3, slices were mounted with Vectashield (Vector Labs, Burlingame, CA) containing nuclear counter-stain (DAPI).

Fluorescence microscopy and quantitative digital imaging analysis

Imaging of slices was performed on an inverted Zeiss Axiovert 200M with 63× plan-apo/1.4 numerical aperture objective, 175 W xenon illumination (Sutter Instruments, Novato, CA), Coolsnap CCD camera (Princeton Instruments, Trenton, NJ), and SlideBook version 4.0–5.0 software (Intelligent Imaging Innovations, Ringsby, CT) as described previously (Smith et al., 2006;Robertson et al., 2009). For detection of indirect immunofluorescence of Alexa 488/568/DAPI, three-dimensional *z*-stack images of *x–y* planes with 0.3 µm steps were collected. Images were deconvolved to the nearest neighbor to generate confocal *x–y* sections. For somatic regions, masks for each *x–y* plane were hand-drawn to exclude non-neuronal elements (glia or vascular) that included as much of CA1 stratum pyramidale as

possible. For apical dendritic regions, masks, drawn on anti-MAP2 images, began > 20 μm from the extreme edge of stratum pyramidale to also exclude non-neuronal elements. Mean fluorescence intensity corresponding to each mask from each channel through all *x*–*y* planes was calculated. The dendritic:somatic ratio was calculated for each channel to allow comparisons between slices with different intensities. The ratio associated with anti-FMRP fluorescence was normalized by dividing by the ratio associated with anti-MAP2 fluorescence to allow comparisons between slices with slightly different neuronal densities. Typically, 3 image fields from 3 slices from each condition were analyzed.

Three-Chamber Social Approach Task

The three-chambered social approach task, employed as a standard test for assaying sociability in mice(Nadler et al., 2004;Moy et al., 2009;Yang et al., 2011), was adapted for rats by scaling the size of the apparatus. Briefly, a subject rat (control or ELS, type blinded to experimenter) was placed into the middle chamber of the divided, 3-chamber (99 (*W*) × 162 (*L*) × 41 cm (*H*)) apparatus. An empty, inverted, plastic, medium-sized, golf-range bucket (Western Golf, Thousand Palms, CA) was placed beforehand in each of the two outer compartments. Initially the subject rat was placed in the center chamber for a ten minute habituation; for this initial habituation phase, the doors to the other compartments were closed. For the second habituation phase, the sliding doors (10 × 10 cm) were elevated and the subject rat given free access to the three chambers during a 10 min session. Following the habituation phases, the subject rat was placed back into the center, the sliding doors were closed and an unfamiliar male target (trained and habituated) rat was placed under one of the two buckets while a novel object was placed under the other bucket; the doors were opened and the subject rat permitted to explore the entire apparatus for 10 min for the sociability phase. The time spent in each compartment during both sessions was collected via video (JVC Everio, Bedford, TX) and scored off-line using TopScan (CleverSys, Reston, VA). The apparatus was cleaned with ethanol (70%) between each rat. White noise (70 dB) with dimmed lighting was present during testing.

Statistics

Data are expressed as mean ± SEM with n = number of rats for a given treatment. Data are plotted using Sigmaplot 12.0 (Systat, Chicago, IL). Mann-Whitney Rank Sum, ANOVA with Bonferroni or Holm-Sidak post-hoc testing, repeated measures ANOVA and Student's t-tests were used, where indicated and appropriate, for statistical comparisons for electrophysiological, immunocytochemical, biochemical and behavioral data using Origin 7.5 S5R (Origin Lab Corporation, Northampton, MA), SPSS (IBM, Armonk, NY) or SigmaStat 3.11 (Systat, Chicago, IL). Outlier analysis (where required – used only for FMRP-P P2 fractions analysis) were performed using Minitab 16 (State College, PA), data points with standardized residuals greater than 3 were further inspected for validity. Significance is reported at $P < 0.05$ unless otherwise nonsignificant (NS).

Results

ELS does not result in an epileptic phenotype at P60

Studies by others (Stafstrom et al., 1993;Galanopoulou, 2008) have failed to find evidence of epilepsy (spontaneous seizures) after subcutaneous kainate injection at P7 (ELS). In order to confirm that our phenotypic observations were not associated with spontaneous seizures, we used combined video-EEG monitoring at P60+ following ELS. We monitored 6 rats following ELS continuously for 5–17 days (average 12 ± 2 days) and made comparisons to 4 saline-injected control rats monitored for 5 days. No discharges of any duration that could be consistent with spontaneous seizures were observed in either group. Diurnal background rhythms in each group appeared qualitatively similar (Supplemental Figure 1).

mLTD is preferentially enhanced chronically following ELS

Since our previous studies found enhanced LTD at P60+ following ELS(Cornejo et al., 2007), we first isolated mLTD with a specific induction protocol (SPP-LFS) in the presence of D-APV(Kemp et al., 2000). We utilized a two-pathway protocol in order to investigate both stimulation-induced and chemical-induced (DHPG) mLTD. We found that both stimulation-induced mLTD (fEPSP slopes, normalized to 100% baseline, ELS: 54.82± 2.52%, n = 12, control: 82.06± 2.55%, n = 8, $P < 0.001$, Student's t-test (Figs. 1A, 3B)) and chemical-induced mLTD (ELS: 55.12± 2.23%, n = 10, control: 72.874± 2.44%, n = 8, $P < 0.001$, Student's t-test, (Fig. 1B)) were significantly enhanced at P60+ following ELS. We further determined the specificity of enhanced mGluR LTD following ELS using the specific mGluR5 antagonist MTEP (I 3-((2-Methyl-4-thiazolyl)ethynyl)pyridine)(Matta et al., 2011;Kwag and Paulsen, 2012). In the presence of D-APV (50 μM), two-pathway protocol was used to investigate stimulation-induced mLTD induction first in the absence of MTEP (Figure 1C, ELS: 57.65±9.73%, n=7, control: 85.41±2.43%, n=7, $P<0.013$, Student's t-test) and then in the presence of MTEP (500nM) (Figure 1D, ELS: 98.282±3.01%, n=6, control: 98.92±4.24%, n=6, P=0.91, Student's t-test). These results confirm that mLTD induction following ELS is indeed mediated by mGluR5, as blocking these receptors prior to induction eliminates all mLTD, while applying the antagonist following induction has no effect on the expression of enhanced mLTD in ELS animals. Further, pathway specificity of mLTD is maintained following ELS. In other words, mLTD remains homosynaptic following ELS.

Next, using a different induction protocol that favors NMDAR-mediated LTD and omitting D-APV (LPP-LFS)(Kemp et al., 2000), we found no significant differences at P60+ following ELS (ELS: 88.82 ± 4.19%, n = 6, control: 89.58 ± 3.16%, n = 7, P = NS, Student's t-test (Figs. 2A, 3B)). The amount of LTD under these conditions was less than that seen for mLTD (Fig. 3B, ANOVA, $P < 0.05$), consistent with less NMDAR-mediated LTD at P60(Dudek and Bear, 1993;Kemp et al., 2000). Taken together, this suggests that ELS preferentially affected the induction and expression of mLTD compared to NMDAR-mediated LTD. Our prior studies(Cornejo et al., 2007) did not find any alterations that could be attributed to chronic changes in presynaptic function following ELS.

mLTD is still protein synthesis dependent following ELS

mLTD induction is critically dependent on protein synthesis (Huber et al., 2000). mLTD becomes protein synthesis independent with genetic loss of FMRP (Osterweil et al., 2010;Nosyreva and Huber, 2006). Since genetic loss of FMRP results in enhanced mLTD (Nosyreva and Huber, 2006;Volk et al., 2007) similar to ELS, we hypothesized that mLTD following ELS might be protein synthesis independent. Therefore, mLTD was measured in the continuous presence of two different protein synthesis inhibitors individually. First, in the presence of anisomycin (20 μM), stimulus induced mLTD was equally reduced following ELS compared to controls (ELS: 94.22 ± 3.82%, n = 6, control: 98.05 ± 2.44%, n = 6, P = NS, Student's t-test (Fig. 2B)). Similarly, in cycloheximide (60 μM) stimulus induced mLTD was equally, but not totally, blocked following ELS compared to controls (ELS: 91.02 ± 5.33%, n = 6, control: 89.58 ± 4.24%, n = 7, P = NS, Student's t-test (Fig. 2C)). Therefore by comparison to stimulus induced mLTD in the absence of protein synthesis inhibitors (Fig. 3B), the enhanced mLTD following ELS remains dependent on protein synthesis. This is similar to what is reported in the FMRP premutation mouse with modest reduction of FMRP expression with modest reduction of FMRP expression (Iliff et al., 2013).

PP2A regulation of mLTD is occluded following ELS

Non-specific blockade of both PP2A and PP1 has previously been shown to enhance mLTD under different conditions(Schnabel et al., 2001). We used okadaic acid (OA) at a concentration (3 nM) that blocks PP2A with relative selectivity over PP1(Swingle et al., 2007). We chose a relatively brief incubation to investigate the effects on activated PP2A and prevent alterations in background phosphorylation and other off-target effects seen with longer treatments(Niere et al., 2012). OA significantly enhanced mLTD in controls (controls with OA: 52.47 ± 4.49%, n = 8, controls without OA: 82.06± 2.55%, n = 8, P = 0.001, Student's t-test (Figs. 1A, 3AB)). Thus, PP2A regulates and limits the amount of mLTD under control conditions. mLTD was similar between controls with OA, ELS with OA (54.09 ± 4.99%, n = 9) and ELS without OA (Figs. 3AB, c.f. Fig 1 A)). Taken together, PP2A regulation of mLTD is lost following ELS since further enhancement of mLTD was not seen with PP2A blockade.

Characterization of phosphorylated FMRP antibody—Since these alterations in mLTD could be due to alterations in FMRP expression and function, it was first necessary to develop an antibody that would detect the different functional states of FMRP. We generated a novel polyclonal antibody (6058) against a peptide corresponding to the primary site of FMRP phosphorylation, S499 (Ceman et al., 2003), (see Methods.) Phosphorylation at S499 is associated with stalled ribosomes (Ceman et al., 2003), while dephosphorylation at S499 is associated with somatodendritic transport(Bassell and Warren, 2008) and ubiquination and proteasomal degradation(Hou et al., 2006;Niere et al., 2012). Treatment of hippocampal slices with DHPG (100 μM × 30 mins) has been shown with a previous antibody to result in robust phosphorylation of FMRP(Narayanan et al., 2008). Similarly, we treated adult hippocampal slices with DHPG and compared them to untreated matched-slice controls. Western-blot analysis revealed that 6058 selectively labeled a band around 75kDa corresponding to the molecular weight of FMRP; intensity of this band was increased by DHPG treatment and completely eliminated by phosphatase treatment (Fig. 4AB), demonstrating that 6058 exclusively recognizes biologically active FMRP phosphoprotein. Immunoprecipitaion of FMRP (7G1 −1) followed by re-blot with 7G1 −1 and 6058 further demonstrated specificity of 6058 for FMRP and preservation of FMRP phosphorylation by our immunoprecipitation protocol (Suppl Fig. 2B). Furthermore, probing FMRP KO mice and S499A mutant FMRP (Fig. 4CD) further demonstrated the specificity of the 6058 antibody for S499 phosphorylated FMRP.

Expression of key mediator proteins of mLTD following ELS

We postulated that exaggerated mLTD seen chronically following ELS might be reflected by dysregulated protein expression of key mediators of mLTD, especially those for which phosphorylation might influence alterations in activity. As a precedent, this has been observed for NMDAR-mediated LTD(Peineau et al., 2007). Theoretically, enhanced mLTD could be influenced by reduced expression of FMRP or PP2A or enhanced expression of mGluR5, the main Group 1 mGluR subtype involved in postsynaptic CA1 hippocampal signaling (Collingridge et al., 2010), or STEP, the tyrosine phosphatase associated with mLTD expression(Zhang et al., 2008). We did not find significant alterations in the expression of FMRP, phosphorylated FMRP, the core, catalytic subunit of PP2A (PP2AC), STEP or mGluR5 (Fig. 5), though a trend towards increased mGluR5 was observed. Prior work suggests that a nearly two fold increase in mGluR5 expression might be needed to explain enhanced mLTD seen following ELS (Huber et al., 2001). However, small increases in mGluR5 expression might explain long-term changes in down-stream signaling influenced by mGluR5 activation. Signaling through Akt occurs both through mGluRs(Collingridge et al., 2010) and NMDARs(Peineau et al., 2007) to balance the expression of LTD via phosphorylating GSK3β on Ser 9, rendering it inactive. Active Akt

(phosphorylated on Ser 473) has been reportedly increased(Sharma et al., 2010), unchanged(Osterweil et al., 2010) and decreased(Hu et al., 2008) in genetic disruptions of FMRP. We did not find significant alterations in the total expression or in the expression of phosphorylated isoforms of Akt (Ser 473) or GSK3β (Ser 9) following ELS compared to controls (Fig. 6). Thus, alterations in basal signaling via mGluRs or NMDARs were less likely to influence alterations in mLTD induction or expression.

S6K is activated (Thr 389 phosphorylation) through mGluR activation to influence the function of FMRP (Narayanan et al., 2008). S6K phosphorylation is increased in genetic disruption of FMRP (Sharma et al., 2010). S6K expression and activation were not altered 2 days after ELS (P9, Fig. 7ab). However, we found an increase in phosphorylated S6K (ELS: 239.51 ± 72.35% of control, $P < 0.05$, Student' s t-test) without alteration of total S6K (ELS: 96.7 ± 10.5% of control)(Fig. 7CD) weeks (P60+) after ELS. While S6K may be initially activated after ELS (Talos et al., 2012), lack of activation 2 days after ELS suggests that S6K activation is not associated with triggering the latent phenotype after ELS. This is consistent with the latent development of abnormal S6K–mediated signaling following ELS and possibly secondary to other signaling pathways. S6, one of the substrates of S6K that directly regulates protein translation (Nygard and Nilsson, 1990) and is activated by mGluR activation (Antion et al., 2008a), showed significantly increased phosphorylation (activation) on Ser 240/244 following ELS at P60+ (ELS: 135.42 ± 8.81% of control, $P< 0.005$, Student's t-test). This is consistent with prolonged activation of S6K (Arechiga et al., 2007). There was no change in total expression of S6 nor did we find changes in phosphorylation of S6 at the Ser 235/236 site, consistent with the notion that S6K does not phosphorylate this site directly (Pende et al., 2004) (Fig. 8) and is not fully activated. Expression of another S6K target and regulator of protein translation, EIF4B was unchanged (Supplemental Figure 3.). These data corroborate our electrophysiological results that demonstrate mGluR LTD is still dependent on protein synthesis in ELS rats(Fig. 2BC, 3B). This is similar to what has been reported in the fragile X premutation mice(Iliff et al., 2013).

Compartmentalization and interaction of FMRP, S6K and PP2AC following ELS

Since neither FMRP nor PP2AC total expression was altered chronically following ELS, we hypothesized that disruption in either their sub-cellular targeting or interactions could underlie the ELS mediated alterations in mLTD. FMRP redistribution is found in the hippocampus after mGluR stimulation(Antion et al., 2008a;Hou et al., 2006;Antar et al., 2004;Nalavadi et al., 2012). Further, FMRP redistribution may be regulated by phosphorylation(Bassell and Warren, 2008). Regulation of PP2A is undoubtedly complex, given that the enzyme can potentially exist in 75 different holoenzyme compositions, but each with PP2AC at the core(Janssens et al., 2005). Given that FMRP, S6K and PP2A have been characterized as dynamic binding partners(Narayanan et al., 2008), disrupted targeting of one should correlate with that of the other. We therefore investigated the compartmentalization of FMRP, PP2AC and S6K following ELS with subcellular fractionation to report a concentration of each protein in each fraction. The concentration of each protein was normalized to control for that fraction. Under control conditions, FMRP, PP2A and S6K were enriched (on average) 1.3, 3.3 and 1.8 fold, respectively, in the cytosolic (S2) fraction compared to the P2 fraction. PSD95 was excluded from cytosolic fractions and enriched in synaptosomal fractions, consistent with appropriate separation(Rockstroh et al., 2011) (Supplemental Figure 4). Following ELS, FMRP was significantly removed from the cytosolic compartment (S2 fraction, ELS: 75.87 ± 5.66%, $n = 12$; control: 100 ± 10.67%, $n = 10$, $P < 0.05$, Student's t-test) (Fig. 9A). FMRP was increased in the nuclear compartment (P1 fraction, ELS: ELS: 160.11 ± 18.60% of control, $P < 0.05$, Student's t-test) Phosphorylated FMRP was reduced in the cytosolic compartment. (ELS: 53.14 ± 12.78% of control, $P< 0.05$, Student's t-test). In parallel with FMRP, PP2AC

was significantly removed from the cytosolic compartment (S2 fraction) (ELS: 66.88 ± 6.30%, n = 11 control: 100 ± 14.32%, n = 10, P < 0.05, Student's t-test)(Fig. 9C). Surprisingly, FMRP expression in P2 (synaptosomal) fractions was not significantly changed following ELS, but there was significantly increased phosphorylated FMRP in the synaptic compartment (ELS: (Fig 9B) (ELS: 208.13% of control, P<0.05, Student's t-test). PP2AC expression in P2 (synaptosomal) fractions was not significantly changed following ELS (Fig 9C). While there were no significant alterations in the distribution of S6K, phosphorylated S6K was reduced in the cytosolic compartment (ELS: 63.13 ± 10.35% of control, P< 0.02, Student's t-test) and increased in the synaptic compartment (ELS: 175.00 ± 38.58% of control, P< 0.05, Student's t-test) (Fig. 10AB). Since FMRP is phosphorylated by S6K, the patterns of phosphorylation and distribution are all consistent. To investigate the interactions of FMRP with S6K and PP2A further, we immunoprecipitated FMRP from CA1 hippocampal lysates and probed for S6K and PP2AC to determine if ELS altered the interaction of FMRP with either S6K or PP2AC. Consistent with fractionation, we found reduced S6K immunoreactivity associated with FMRP following ELS (ELS: 65.52 ± 11.63%, n = 7; control: 100 ± 10.22%, n = 8, P < 0.05, Student's t-test) (Fig. 11A). PP2AC immunoreactivity associated with FMRP was unchanged by ELS (ELS: 101.77 ± 7.93%, n = 7; control: 100 ± 5.17%, n = 7, P = NS, Student's t-test) (Fig. 11A). Therefore, the parallel shifts in FMRP and PP2AC from the cytosolic fraction are correlated with their binding interactions. This suggests that ELS alters the FMRP complex to selectively reduce S6K binding to FMRP while PP2Ac binding is maintained(Narayanan et al., 2008). Further, since FMRP favors PP2A binding over S6K when de-phosphorylated (Narayanan et al., 2008) this is consistent with conditions caused by ELS to favor selective redistribution of PP2A and FMRP without S6K from the cytosolic compartment.

We then investigated the compartmentalization of STEP. STEP translation is mediated directly by FMRP (Darnell et al., 2011). STEP translation and activation directly mediates mLTD expression (Moult et al., 2006;Zhang et al., 2008). STEP expression is selectively increased post-synaptically in FMRP knock-out mice (Goebel-Goody et al., 2012). Following activation, STEP targets AMPAR for removal from the synapse via dephosphorylation(Zhang et al., 2008). At weeks (P60+) following ELS we found a significant two-fold increase in synaptosomal STEP (ELS: 218.95 ± 51.05, n = 7; control: 100 ± 21.16, n = 8, P = 0.042, Student's t-test) (Fig. 11B). We did not find any significant change in levels of cytosolic STEP (ELS 123.40 ± 17.70, n = 7; control: 100 ± 15.51, n = 7, P = 0.340, Student's t-test). Given that alterations in STEP expression have been shown to directly influence the expression of plasticity (Pelkey et al., 2002), this identifies a primary mechanism by which deficits in FMRP function following ELS result in enhanced mLTD expression (Supplemental Figure 5). More synaptosomal STEP is consistent with a greater number of AMPA receptors being dephosphorylated, and subsequently internalized following mLTD induction(Zhang et al., 2008) in order to mediate mLTD expression.

Altered Localization of FMRP following ELS

In order to confirm the shift of FMRP seen with subcellular fractionation following ELS, we visualized this change using immunocytochemistry and fluorescence microscopy. In CA1, anti-FMRP staining was diffusely clustered around neuronal somata and puncta along anti-MAP2 stained dendrites in stratum radiatum (Fig. 12A). Dendritic puncta are presumed polyribosomal clusters(Stefani et al., 2004;Antar et al., 2005). Non-neuronal elements, due to lack of MAP-2 staining, were also rarely observed but had some anti-FMRP staining (Fig. 12). Following ELS, anti-FMRP staining is shifted from puncta in dendrites to a homogeneous peri-nuclear pattern (Fig. 12BC). Faint anti-FMRP staining is still observed along dendrites, presumably consistent with minimal changes in synaptic pools observed with subcellular fractionation (Fig. 9A). Loss of mRNA granules is also seen in FMRP

knock-out mice(Aschrafi et al., 2005). Anti-FMRP staining in non-neuronal elements appears unaffected.

Altered sociability following ELS

Our prior studies (Cornejo et al., 2007;Cornejo et al., 2008) found that adult rodents have impaired hippocampal-dependent learning and memory following ELS. We also found abnormalities in fear conditioning (Cornejo et al., 2008) that are consistent with an autistic phenotype and similar to the exaggerated responses seen in another rat model of autism (Markram et al., 2008). Given the association of genetic loss of FMRP with an autistic phenotype (Mineur et al., 2006;Spencer et al., 2005), we examined a behavioral feature linked to autistic phenotypes, abnormal sociability, using the three-chambered social approach task in adult rats. During the habituation phase (trial #2, Methods), neither control or ELS rats demonstrated a preference for any of the three chambers (P=0.48, two way ANOVA) (Fig. 13A) and confirming no side preferences and validating the empty apparatus. During trial #3, the sociability phase, ELS rats displayed a reduced preference for spending time in the “novel rat” chamber (control: 537.86±33.40 s, n=9, ELS: 393.80±27.95 s, n=11, P=0.002, two way ANOVA, Holm-Sidak post-hoc comparisons)(Fig. 13B). These abnormalities in the three chamber social interaction task are consistent with autistic features after ELS and other rodent models of autism (Silverman et al., 2010;Crawley, 2007). Given our prior findings of normal open field and elevated plus maze testing following ELS (Cornejo et al., 2008), it is unlikely that alterations in activity or anxiety, as measured by these tests, contributed to our findings.

Discussion

We have demonstrated that the chronically enhanced LTD following ELS is specifically mediated by mGluRs (mLTD), similar to that seen with genetic disruption of FMRP. We subsequently investigated the expression of proteins associated with mLTD and FMRP signaling. FMRP, S6K and PP2A are thought to cooperate as a signaling complex (Narayanan et al., 2007;Narayanan et al., 2008). While we find no changes in FMRP and PP2A total expression, S6K is hyperphosphorylated, consistent with S6K overactivation. Since this and Akt overactivation (which we did not observe) are seen in genetic loss of FMRP (Sharma et al., 2010), we postulated that more nuanced alterations of the FMRP complex such as redistribution of FMRP away from synapses could explain our findings. Surprisingly, we found that FMRP and PP2A are unchanged in synaptic compartments but removed from cytosolic (non-synaptic) compartments in adult rats following ELS. This was surprising because synaptic compartments are the presumed locus for mLTD induction and expression. Since the total amounts and the synaptic fractions of FMRP and PP2A were unchanged by ELS, the loss of FMRP and PP2A from the cytosolic compartment would be consistent with redistribution of both proteins from the non-synaptic/cytosolic compartment in dendrites towards the somatic compartment, which was supported by imaging. Further supporting the mechanistic importance of their re-distribution, ELS occluded PP2A mediated regulation of mLTD.

Binding of FMRP to PP2A remains intact following ELS, (but with reduced bound S6K) supporting their joint redistribution and consistent with reports describing their collective interactions, including those dependent on FMRP phosphorylation (Narayanan et al., 2008). The reduction of S6K binding to FMRP is noteworthy, as it is speculated that S6K rephosphorylates FMRP, thus resetting its ability to inhibit protein translation (Ceman et al., 2003) and thus limit mLTD (Antion et al., 2008b). The reduced association of FMRP and S6K corroborates that FMRP is not being rephosphorylated effectively and specifically in the cytosolic compartment, which could locally influence protein translation, FMRP transport(Bassell and Warren, 2008) and degradation(Hou et al., 2006;Niere et al., 2012).

Indeed, we find correlations in FMRP phosphorylation with S6K activation such that FMRP phosphorylation is reduced in the cytosolic compartment concurrently with a reduction in activated S6K and vice-versa in the synaptic compartment. Our findings illustrate new aspects of FMRP signaling that cannot be explored using traditional knock-out approaches as they are location dependent. Thus, FMRP dysfunction, short of genetic loss, also underlies deregulation of mLTD.

Investigation of STEP, a protein whose translation is dynamically limited by FMRP(Darnell et al., 2011), indicated that STEP expression is significantly increased in the synaptosomal fraction following ELS. STEP expression is selectively increased post-synaptically in FMRP knock-out mice(Goebel-Goody et al., 2012). In our prior work, we also found another FMRP target (Brown et al., 2001) with altered synaptosomal expression after ELS, PSD95(Cornejo et al., 2007). This clarifies the mechanism(s) by which impaired FMRP function following ELS underlies enhanced mLTD (Supplemental Figure 5). Specifically, increased levels of synaptic STEP may result in more AMPARs being targeted for removal from the synapse via dephosphorylation (Zhang et al., 2008), i.e., enhanced mLTD expression (Pelkey et al., 2002).

The specific location of protein synthesis for mLTD as mediated by FMRP is not completely clear, though presumed to be very near synapses and the site of mLTD expression. Polyribosomes are located both throughout dendrites and in clusters at the base of spines(Antar et al., 2005). Most FMRP (80–90%) is associated with polyribosomes and present at the base of spines(Stefani et al., 2004). Given that protein synthesis was intact following ELS to mediate mLTD and that FMRP (and PP2AC) concentrations in synaptic fractions were surprisingly unchanged, this suggests that synaptic protein synthesis is not disrupted following ELS. Thus, mLTD *induction* is intact following ELS. Given the reduction of FMRP and PP2A from non-synaptic compartments and the associated enhancement of mLTD following ELS, these findings support a role of non-synaptic compartments and, possibly, inter-compartmental signaling by FMRP and PP2A in regulating mLTD *expression* under normal conditions. Consistent with our data, dephosphorylated FMRP redistributes away from synapses along the nuclear-dendritic axis (Antar et al., 2004), however the role and specifics of FMRP redistribution seen with mLTD have not previously been demonstrated. It is possible that once synaptic FMRP (and potentially other associated proteins) are dephoshorylated and removed from the ribosome, these proteins are degraded (Hou et al., 2006;Nalavadi et al., 2012), and “new” FMRP/PP2A/S6K complexes are drawn to the synapse from pools in the cytoplasm in order to replace the FMRP “brake” on local translation. Following ELS, these “pools” in the cytoplasm are lacking. This would explain why mLTD following ELS is still protein synthesis dependent, yet is still influenced by FMRP dysfunction (Supplemental Figure 5). Furthermore, this highlights the important role of the FMRP complex as a biphasic modulator of mLTD, as it involves the regulation of protein synthesis.

Genetic removal of S6K1 corrects molecular, synaptic and behavioral aspects caused by loss of FMRP(Bhattacharya et al., 2012). Our data are consistent with S6K being a key modulator of FMRP function. This supports the mechanism suggested by our data where the interactions of FMRP, PP2A and S6K are coordinated, and subsequently disrupted by ELS, to biphasically regulate mLTD. This proposed motif of FMRP (Narayanan et al., 2008) is similar to that of AKAP79/150, a mobile synapto-dendritic protein that binds both kinases and phosphatases to regulate plasticity (Sanderson and Dell’Acqua, 2011). Consistent with our data, evidence suggests that phosphorylation of FMRP favors S6K binding over PP2A and conversely dephosphorylation favors PP2A over S6K(Narayanan et al., 2008), though other modifications of FMRP have also been proposed (Blackwell et al., 2010).

Given that PP2A is needed to activate FMRP and protein translation, it might be expected that PP2A blockade would limit mLTD induction (Niere et al., 2012). However, our findings support a role for PP2A in regulating mLTD expression and are consistent with a prior report (Schnabel et al., 2001). We utilized a concentration of OA which should be very specific for PP2A over PP1 (Swingle et al., 2007). However, use of any PP2A antagonist potentially implicates all of the phosphorylated proteins regulated by PP2A in addition to FMRP. PP2A regulation of mLTD that was completely occluded by ELS supports two important conclusions. First, PP2A localization is important in regulating mLTD and second, PP2A regulation of mLTD likely influences mLTD expression outside of its modulation of FMRP, possibly down-stream from protein translation (Supplemental Figure 5). Taken together, the linked and parallel disruptions of FMRP and PP2A localization following ELS and the associated alterations mediated by PP2A blockade on mLTD support a role for the FMRP-PP2A–S6K complex in regulating mLTD.

Importantly, it remains unclear how the chronic changes found at P60+ evolved from ELS at P7. Our data supports that this is not an immediate consequence of ELS but rather it results from an altered developmental trajectory. This is based on our findings of latent hyperphosphorylation of S6K after P9. It suggests that a therapeutic window exists in which these long term changes may be circumvented. Studies by others (Stafstrom et al., 1993;Galanopoulou, 2008) and our studies here have failed to find evidence of epilepsy (spontaneous seizures) at P60+ following ELS in this model. There are many differences here compared to the hypoxia model of ELS (Talos et al., 2012), including lack of epilepsy (Rakhade et al., 2011), where S6K activation has been implicated in the triggering process. Thus having excluded epilepsy and S6K activation, it is not immediately clear how these changes are activated and maintained. In this model of ELS, there is no evidence of overt cellular damage to the hippocampus, such as cell loss (Nitecka et al., 1984;Lynch et al., 2000;Wirrell et al., 2001), sprouting (Holmes, 1991;Cornejo et al., 2007) or alterations in spine numbers (Cornejo et al., 2007) to suggest structural mechanisms that may underlie the alterations in mLTD. This is in contrast to repeated ELS models where structural abnormalities have been shown(Sogawa et al., 2001;Nishimura et al., 2011). In prior studies, loss of long-term potentiation (LTP) in adult rats after ELS was attributed to alterations in GABAergic tone in the dentate gyrus (Lynch et al., 2000) and reduced expression of GluN2A in CA1(Cornejo et al., 2007). Indeed, loss of FMRP function has been linked to reduction of hippocampal LTP (Hu et al., 2008;Lauterborn et al., 2007) and homeostatic plasticity (Soden and Chen, 2010). Studies here now support enhanced post-synaptic STEP expression, as seen in over-expression studies (Pelkey et al., 2002), as a major contributor to the loss of LTP after ELS.

Determining pharmacologically which targets may normalize mLTD following ELS are critical for future studies in order to determine if these may influence the abnormal behavioral phenotype, which includes alterations in learning and memory, observed after ELS (Cornejo et al., 2007;Cornejo et al., 2008;Lynch et al., 2000;Sayin et al., 2004). We have identified FMRP signaling related targets; however it is very possible that other distinct signaling pathways are affected. Our findings of altered socialization now further link ELS with symptoms associated with autism and a phenotype with ID. While many studies have explored the core features of autism in genetically modified mice (Silverman et al., 2010), these have not yet been extended to rats, an area of further study. Exaggerated fear responses (Markram et al., 2008) and altered socialization (Bambini-Junior et al., 2011), identical to our findings after ELS (Cornejo et al., 2008), are seen in the best known rat model of autism, *in utero* valproic acid exposure. These findings direct future studies that may have important consequences for clinical treatments for disorders with intellectual disability and autistic features outside of FXS, particularly those associated with ELS or similar early life insults, where abnormal FMRP-mediated signaling may be present.

Supplementary Material

Refer to Web version on PubMed Central for supplementary material.

Acknowledgments

Special thanks to, Ulli Bayer, Mark Dell'Acqua, Steve Coultrap and other members of the Benke, Bayer and Dell'Acqua labs, Ms Vivian Carlson and Ms Christy Beitzel for behavioral analysis, Dr Yogi Raol and the UC Rodent In Vivo Neurophysiology Core, the IDDRC behavior core, the UC Pharmacology Microscopy Core and Dr Tom Finger and the UC CDB Microscopy core. Thanks to Dr. Stephen Warren, Emory University, for supplying the FMRP-wild-type and S499A-FMR1 plasmids. Funding provided by the Children's Hospital Colorado Research Institute, Epilepsy Foundation, and NIH-NINDS (R01 NS076577). The content is solely the responsibility of the authors and does not necessarily represent the official views of NINDS or NIH.

References

Anderson WW, Collingridge GL. The LTP program: a data acquistion program for on-line analysis of long-term potentiation and other synaptic events. J Neurosci Methods. 2001; 108:71–83. [PubMed: 11459620]

Antar LN, Afroz R, Dictenberg JB, Carroll RC, Bassell GJ. Metabotropic glutamate receptor activation regulates fragile x mental retardation protein and FMR1 mRNA localization differentially in dendrites and at synapses. J Neurosci. 2004; 24:2648–2655. [PubMed: 15028757]

Antar LN, Dictenberg JB, Plociniak M, Afroz R, Bassell GJ. Localization of FMRP-associated mRNA granules and requirement of microtubules for activity-dependent trafficking in hippocampal neurons. Genes Brain Behav. 2005; 4:350–359. [PubMed: 16098134]

Antion MD, Hou L, Wong H, Hoeffer CA, Klann E. mGluR-dependent long-term depression is associated with increased phosphorylation of S6 and synthesis of elongation factor 1A but remains expressed in S6K–deficient mice. Mol Cell Biol. 2008a; 28:2996–3007. [PubMed: 18316404]

Antion MD, Merhav M, Hoeffer CA, Reis G, Kozma SC, Thomas G, Schuman EM, Rosenblum K, Klann E. Removal of S6K1 and S6K2 leads to divergent alterations in learning, memory, and synaptic plasticity. Learn Mem. 2008b; 15:29–38. [PubMed: 18174371]

Arechiga AF, Bell BD, Leverrier S, Weist BM, Porter M, Wu Z, Kanno Y, Ramos SJ, Ong ST, Siegel R, Walsh CM. A Fas-associated death domain protein/caspase-8-signaling axis promotes S-phase entry and maintains S6 kinase activity in T cells responding to IL-2. J Immunol. 2007; 179:5291–5300. [PubMed: 17911615]

Aschrafi A, Cunningham BA, Edelman GM, Vanderklish PW. The fragile X mental retardation protein and group I metabotropic glutamate receptors regulate levels of mRNA granules in brain. Proc Natl Acad Sci U S A. 2005; 102:2180–2185. [PubMed: 15684045]

Bambini-Junior V, Rodrigues L, Behr GA, Moreira JC, Riesgo R, Gottfried C. Animal model of autism induced by prenatal exposure to valproate: behavioral changes and liver parameters. Brain Res. 2011; 1408:8–16. [PubMed: 21767826]

Bassell GJ, Warren ST. Fragile X syndrome: loss of local mRNA regulation alters synaptic development and function. Neuron. 2008; 60:201–214. [PubMed: 18957214]

Bhattacharya A, Kaphzan H, Alvarez-Dieppa AC, Murphy JP, Pierre P, Klann E. Genetic removal of p70 S6 kinase 1 corrects molecular, synaptic, and behavioral phenotypes in fragile X syndrome mice. Neuron. 2012; 76:325–337. [PubMed: 23083736]

Blackwell E, Zhang X, Ceman S. Arginines of the RGG box regulate FMRP association with polyribosomes and mRNA. Hum Mol Genet. 2010; 19:1314–1323. [PubMed: 20064924]

Brown V, Jin P, Ceman S, Darnell JC, O'Donnell WT, Tenenbaum SA, Jin X, Feng Y, Wilkinson KD, Keene JD, Darnell RB, Warren ST. Microarray identification of FMRP-associated brain mRNAs and altered mRNA translational profiles in fragile X syndrome. Cell. 2001; 107:477–487. [PubMed: 11719188]

Buchmayer S, Johansson S, Johansson A, Hultman CM, Sparen P, Cnattingius S. Can association between preterm birth and autism be explained by maternal or neonatal morbidity? Pediatrics. 2009; 124:e817–e825. [PubMed: 19841112]

Ceman S, O'Donnell WT, Reed M, Patton S, Pohl J, Warren ST. Phosphorylation influences the translation state of FMRP-associated polyribosomes. Hum Mol Genet. 2003; 12:3295–3305. [PubMed: 14570712]

Collingridge GL, Peineau S, Howland JG, Wang YT. Long-term depression in the CNS. Nat Rev Neurosci. 2010; 11:459–473. [PubMed: 20559335]

Cornejo BJ, Mesches MH, Benke TA. A single early-life seizure impairs short-term memory but does not alter spatial learning, recognition memory, or anxiety. Epilepsy Behav. 2008; 13:585–592. [PubMed: 18678283]

Cornejo BJ, Mesches MH, Coultrap S, Browning MD, Benke TA. A single episode of neonatal seizures permanently alters glutamatergic synapses. Ann Neurol. 2007; 61:411–426. [PubMed: 17323345]

Crawley JN. Mouse behavioral assays relevant to the symptoms of autism. Brain Pathol. 2007; 17:448–459. [PubMed: 17919130]

Darnell JC, Van Driesche SJ, Zhang C, Hung KY, Mele A, Fraser CE, Stone EF, Chen C, Fak JJ, Chi SW, Licatalosi DD, Richter JD, Darnell RB. FMRP stalls ribosomal translocation on mRNAs linked to synaptic function and autism. Cell. 2011; 146:247–261. [PubMed: 21784246]

Dingledine R, Borges K, Bowie D, Traynelis SF. The glutamate receptor ion channel. Pharmacol Rev. 1999; 51:7–61. [PubMed: 10049997]

Dudek SM, Bear MF. Bidirectional long-term modification of synaptic effectiveness in the adult and immature hippocampus. J Neurosci. 1993; 13:2910–2918. [PubMed: 8331379]

Dzhala VI, Talos DM, Sdrulla DA, Brumback AC, Mathews GC, Benke TA, Delpire EJ, Jensen FE, Staley KJ. NKCC1 transporter facilitates seizures in the developing brain. Nat Med. 2005; 11:1205–1213. [PubMed: 16227993]

Fatemi SH, Folsom TD. Dysregulation of fragile x mental retardation protein and metabotropic glutamate receptor 5 in superior frontal cortex of individuals with autism: a postmortem brain study. Mol Autism. 2011; 2:6. [PubMed: 21548960]

Galanopoulou AS. Dissociated gender-specific effects of recurrent seizures on GABA signaling in CA1 pyramidal neurons: role of GABA(A) receptors. J Neurosci. 2008; 28:1557–1567. [PubMed: 18272677]

Gladding CM, Fitzjohn SM, Molnar E. Metabotropic glutamate receptor-mediated long-term depression: molecular mechanisms. Pharmacol Rev. 2009; 61:395–412. [PubMed: 19926678]

Goebel-Goody SM, Wilson-Wallis ED, Royston S, Tagliatela SM, Naegele JR, Lombroso PJ. Genetic manipulation of STEP reverses behavioral abnormalities in a fragile X syndrome mouse model. Genes Brain Behav. 2012; 11:586–600. [PubMed: 22405502]

Grosshans DR, Browning MD. Protein kinase C activatio induces tyrosine phosphorylation of the NR2A and NR2B subunits of the NMDA receptor. J Neurochem. 2001; 76:737–744. [PubMed: 11158244]

Hagerman R, Hoem G, Hagerman P. Fragile X and autism: Intertwined at the molecular level leading to targeted treatments. Mol Autism. 2010; 1:12. [PubMed: 20858229]

Holmes GL. The long-term effects of seizures on the developing brain: clinical and laboratory issues. Brain Dev. 1991; 13:393–409. [PubMed: 1810153]

Hou L, Antion MD, Hu D, Spencer CM, Paylor R, Klann E. Dynamic translational and proteasomal regulation of fragile X mental retardation protein controls mGluR-dependent long-term depression. Neuron. 2006; 51:441–454. [PubMed: 16908410]

Hu H, Qin Y, Bochorishvili G, Zhu Y, van Aelst L, Zhu JJ. Ras signaling mechanisms underlying impaired GluR1-dependent plasticity associated with fragile X syndrome. J Neurosci. 2008; 28:7847–7862. [PubMed: 18667617]

Huber KM, Kayser MS, Bear MF. Role for rapid dendritic protein synthesis in hippocampal mGluR-dependent long-term depression. Science. 2000; 288:1254–1257. [PubMed: 10818003]

Huber KM, Roder JC, Bear MF. Chemical induction of mGluR5- and protein synthesis--dependent long-term depression in hippocampal area CA1. J Neurophysiol. 2001; 86:321–325. [PubMed: 11431513]

Iliff AJ, Renoux AJ, Krans A, Usdin K, Sutton MA, Todd PK. Impaired activity-dependent FMRP translation and enhanced mGluR-dependent LTD in Fragile X premutation mice. Hum Mol Genet. 2013; 22:1180–1192. [PubMed: 23250915]

Iossifov I, et al. De novo gene disruptions in children on the autistic spectrum. Neuron. 2012; 74:285–299. [PubMed: 22542183]

Janssens V, Goris J, Van Hoof C. PP2A: the expected tumor suppressor. Curr Opin Genet Dev. 2005; 15:34–41. [PubMed: 15661531]

Kemp N, McQueen J, Faulkes S, Bashir ZI. Different forms of LTD in the CA1 region of the hippocampus: role of age and stimulus protocol. Eur J Neurosci. 2000; 12:360–366. [PubMed: 10651891]

Kuenzi FM, Fitzjohn SM, Morton RM, Collingridge GL, Seabrook GR. Reduced long-term potentiation in hippocampal slices prepared using sucrose-based artificial cerebrospinal fluid. J Neurosci Methods. 2000; 100:117–122. [PubMed: 11040373]

Kwag J, Paulsen O. Gating of NMDA receptor-mediated hippocampal spike timing-dependent potentiation by mGluR5. Neuropharmacol. 2012; 63:701–709.

Lauterborn JC, Rex CS, Kramar E, Chen LY, Pandyarajan V, Lynch G, Gall CM. Brain-derived neurotrophic factor rescues synaptic plasticity in a mouse model of fragile X syndrome. J Neurosci. 2007; 27:10685–10694. [PubMed: 17913902]

Luscher C, Huber KM. Group 1 mGluR-dependent synaptic long-term depression: mechanisms and implications for circuitry and disease. Neuron. 2010; 65:445–459. [PubMed: 20188650]

Lynch M, Sayin U, Bownds J, Janumpalli S, Sutula T. Long-term consequences of early postnatal seizures on hippocampal learning and plasticity. Eur J Neurosci. 2000; 12:2252–2264. [PubMed: 10947804]

Markram K, Rinaldi T, La Mendola D, Sandi C, Markram H. Abnormal fear conditioning and amygdala processing in an animal model of autism. Neuropsychopharmacology. 2008; 33:901–912. [PubMed: 17507914]

Matta JA, Ashby MC, Sanz-Clemente A, Roche KW, Isaac JT. mGluR5 and NMDA Receptors Drive the Experience- and Activity-Dependent NMDA Receptor NR2B to NR2A Subunit Switch. Neuron. 2011; 70:339–351. [PubMed: 21521618]

McBride MC, Laroia N, Guillet R. Electrographic seizures in neonates correlate with poor neurodevelopmental outcome. Neurology. 2000; 55:506–513. [PubMed: 10953181]

Miller SP, Weiss J, Barnwell A, Ferriero DM, Latal-Hajnal B, Ferrer-Rogers A, Newton N, Partridge JC, Glidden DV, Vigneron DB, Barkovich AJ. Seizure-associated brain injury in term newborns with perinatal asphyxia. Neurology. 2002; 58:542–548. [PubMed: 11865130]

Mineur YS, Huynh LX, Crusio WE. Social behavior deficits in the Fmr1 mutant mouse. Behav Brain Res. 2006; 168:172–175. [PubMed: 16343653]

Moult PR, Gladding CM, Sanderson TM, Fitzjohn SM, Bashir ZI, Molnar E, Collingridge GL. Tyrosine phosphatases regulate AMPA receptor trafficking during metabotropic glutamate receptor-mediated long-term depression. J Neurosci. 2006; 26:2544–2554. [PubMed: 16510732]

Moy SS, Nadler JJ, Young NB, Nonneman RJ, Grossman AW, Murphy DL, D'Ercole AJ, Crawley JN, Magnuson TR, Lauder JM. Social approach in genetically engineered mouse lines relevant to autism. Genes Brain Behav. 2009; 8:129–142. [PubMed: 19016890]

Nadler JJ, Moy SS, Dold G, Trang D, Simmons N, Perez A, Young NB, Barbaro RP, Piven J, Magnuson TR, Crawley JN. Automated apparatus for quantitation of social approach behaviors in mice. Genes Brain Behav. 2004; 3:303–314. [PubMed: 15344923]

Nalavadi VC, Muddashetty RS, Gross C, Bassell GJ. Dephosphorylation-Induced Ubiquitination and Degradation of FMRP in Dendrites: A Role in Immediate Early mGluR-Stimulated Translation. J Neurosci. 2012; 32:2582–2587. [PubMed: 22357842]

Narayanan U, Nalavadi V, Nakamoto M, Pallas DC, Ceman S, Bassell GJ, Warren ST. FMRP phosphorylation reveals an immediate-early signaling pathway triggered by group I mGluR and mediated by PP2A. J Neurosci. 2007; 27:14349–14357. [PubMed: 18160642]

Narayanan U, Nalavadi V, Nakamoto M, Thomas G, Ceman S, Bassell GJ, Warren ST. S6K1 phosphorylates and regulates fragile X mental retardation protein (FMRP) with the neuronal

protein synthesis-dependent mammalian target of rapamycin (mTOR) signaling cascade. J Biol Chem. 2008; 283:18478–18482. [PubMed: 18474609]

Niere F, Wilkerson JR, Huber KM. Evidence for a fragile x mental retardation protein-mediated translational switch in metabotropic glutamate receptor-triggered arc translation and long-term depression. J Neurosci. 2012; 32:5924–5936. [PubMed: 22539853]

Nishimura M, Gu X, Swann JW. Seizures in early life suppress hippocampal dendrite growth while impairing spatial learning. Neurobiol Dis. 2011; 44:205–214. [PubMed: 21777677]

Nitecka L, Tremblay E, Charton G, Bouillot JP, Berger ML, Ben-Ari Y. Maturation of kainic acid seizure-brain damage in the rat. II. Histopathological sequelae. Neuroscience. 1984; 13:1073–1094. [PubMed: 6527790]

Nosyreva ED, Huber KM. Metabotropic receptor-dependent long-term depression persists in the absence of protein synthesis in the mouse model of fragile X syndrome. J Neurophysiol. 2006; 95:3291–3295. [PubMed: 16452252]

Nygard O, Nilsson L. Translational dynamics. Interactions between the translational factors, tRNA and ribosomes during eukaryotic protein synthesis. Eur J Biochem. 1990; 191:1–17. [PubMed: 2199194]

Ortibus EL, Sum JM, Hahn JS. Predictive value of EEG for outcome and epilepsy following neonatal seizures. Electroencephalogr Clin Neurophysiol. 1996; 99:175–185. [PubMed: 8631277]

Osterweil EK, Krueger DD, Reinhold K, Bear MF. Hypersensitivity to mGluR5 and ERK1/2 leads to excessive protein synthesis in the hippocampus of a mouse model of fragile X syndrome. J Neurosci. 2010; 30:15616–15627. [PubMed: 21084617]

Peineau S, Taghibiglou C, Bradley C, Wong TP, Liu L, Lu J, Lo E, Wu D, Saule E, Bouschet T, Matthews P, Isaac JT, Bortolotto ZA, Wang YT, Collingridge GL. LTP inhibits LTD in the hippocampus via regulation of GSK3beta. Neuron. 2007; 53:703–717. [PubMed: 17329210]

Pelkey KA, Askalan R, Paul S, Kalia LV, Nguyen TH, Pitcher GM, Salter MW, Lombroso PJ. Tyrosine phosphatase STEP is a tonic brake on induction of long-term potentiation. Neuron. 2002; 34:127–138. [PubMed: 11931747]

Pende M, Um SH, Mieulet V, Sticker M, Goss VL, Mestan J, Mueller M, Fumagalli S, Kozma SC, Thomas G. S6K1(−/−)/S6K2(−/−) mice exhibit perinatal lethality and rapamycin-sensitive 5'-terminal oligopyrimidine mRNA translation and reveal a mitogen-activated protein kinase-dependent S6 kinase pathway. Mol Cell Biol. 2004; 24:3112–3124. [PubMed: 15060135]

Rakhade SN, Klein PM, Huynh T, Hilario-Gomez C, Kosaras B, Rotenberg A, Jensen FE. Development of later life spontaneous seizures in a rodent model of hypoxia-induced neonatal seizures. Epilepsia. 2011; 52:753–765. [PubMed: 21366558]

Raol YH, Lund IV, Bandyopadhyay S, Zhang G, Roberts DS, Wolfe JH, Russek SJ, Brooks-Kayal AR. Enhancing GABA(A) receptor alpha 1 subunit levels in hippocampal dentate gyrus inhibits epilepsy development in an animal model of temporal lobe epilepsy. J Neurosci. 2006; 26:11342–11346. [PubMed: 17079662]

Robertson HR, Gibson ES, Benke TA, Dell'Acqua ML. Regulation of postsynaptic structure and function by an A-kinase anchoring protein-membrane-associated guanylate kinase scaffolding complex. J Neurosci. 2009; 29:7929–7943. [PubMed: 19535604]

Rockstroh M, Muller SA, Jende C, Kershner A, von Bergen M, Tomm JA. Cell fractionation- an important tool for compartmental proteomics. J Integr OMICS. 2011; 1:135–143.

Saemundsen E, Ludvigsson P, Hilmarsdottir I, Rafnsson V. Autism spectrum disorders in children with seizures in the first year of life - a population-based study. Epilepsia. 2007; 48:1724–1730. [PubMed: 17555525]

Sanderson JL, Dell'Acqua ML. AKAP signaling complexes in regulation of excitatory synaptic plasticity. Neuroscientist. 2011; 17:321–336. [PubMed: 21498812]

Sayin U, Sutula TP, Stafstrom CE. Seizures in the developing brain cause adverse long-term effects on spatial learning and anxiety. Epilepsia. 2004; 45:1539–1548. [PubMed: 15571512]

Schnabel R, Kilpatrick IC, Collingridge GL. Protein phosphatase inhibitors facilitate DHPG-induced LTD in the CA1 region of the hippocampus. Br J Pharmacol. 2001; 132:1095–1101. [PubMed: 11226140]

Sharma A, Hoeffer CA, Takayasu Y, Miyawaki T, McBride SM, Klann E, Zukin RS. Dysregulation of mTOR signaling in fragile X syndrome. J Neurosci. 2010; 30:694–702. [PubMed: 20071534]

Silverman JL, Yang M, Lord C, Crawley JN. Behavioural phenotyping assays for mouse models of autism. Nat Rev Neurosci. 2010; 11:490–502. [PubMed: 20559336]

Smith KE, Gibson ES, Dell'Acqua ML. cAMP-dependent protein kinase postsynaptic localization regulated by NMDA receptor activation through translocation of an A-kinase anchoring protein scaffold protein. J Neurosci. 2006; 26:2391–2402. [PubMed: 16510716]

Soden ME, Chen L. Fragile X protein FMRP is required for homeostatic plasticity and regulation of synaptic strength by retinoic acid. J Neurosci. 2010; 30:16910–16921. [PubMed: 21159962]

Sogawa Y, Monokoshi M, Silveira DC, Cha B-H, Cilio MR, McCabe BK, Liu X, Holmes GL. Timing of congnitive deficits following neonatal seizures: relationship to histological changes in the hippocampus. 2001:73–83.

Spencer CM, Alekseyenko O, Serysheva E, Yuva-Paylor LA, Paylor R. Altered anxiety-related and social behaviors in the Fmr1 knockout mouse model of fragile X syndrome. Genes Brain Behav. 2005; 4:420–430. [PubMed: 16176388]

Stafstrom CE, Chronopoulos A, Thurber S, Thompson JL, Holmes GL. Age-dependent cognitive and behavioral deficits after kainic acid seizures. Epilepsia. 1993; 34:420–432. [PubMed: 8504777]

Stefani G, Fraser CE, Darnell JC, Darnell RB. Fragile X mental retardation protein is associated with translating polyribosomes in neuronal cells. J Neurosci. 2004; 24:7272–7276. [PubMed: 15317853]

Swingle M, Ni L, Honkanen RE. Small-molecule inhibitors of ser/thr protein phosphatases: specificity, use and common forms of abuse. Methods Mol Biol. 2007; 365:23–38. [PubMed: 17200551]

Talos DM, Sun H, Zhou X, Fitzgerald EC, Jackson MC, Klein PM, Lan VJ, Joseph A, Jensen FE. The interaction between early life epilepsy and autistic-like behavioral consequences: a role for the mammalian target of rapamycin (mTOR) pathway. PLoS One. 2012; 7:e35885. [PubMed: 22567115]

Tremblay E, Nitecka L, Berger ML, Ben-Ari Y. Maturation of kainic acid seizure-brain damage syndrome in the rat. I. Clinical, electrographic and metabolic observations. Neuroscience. 1984; 13:1051–1072. [PubMed: 6527789]

Tuchman R, Moshe SL, Rapin I. Convulsing toward the pathophysiology of autism. Brain Dev. 2009; 31:95–103. [PubMed: 19006654]

Volk LJ, Pfeiffer BE, Gibson JR, Huber KM. Multiple Gq-coupled receptors converge on a common protein synthesis-dependent long-term depression that is affected in fragile X syndrome mental retardation. J Neurosci. 2007; 27:11624–11634. [PubMed: 17959805]

Wirrell EC, Armstrong EA, Osman LD, Yager JY. Prolonged seizures exacerbate perinatal hypoxic-ischemic brain damage. Pediatr Res. 2001; 50:445–454. [PubMed: 11568286]

Yang M, Silverman JL, Crawley JN. Automated three-chambered social approach task for mice. Curr Protoc Neurosci. 2011; 56:8.26.1–8.26.16.

Zhang Y, Venkitaramani DV, Gladding CM, Zhang Y, Kurup P, Molnar E, Collingridge GL, Lombroso PJ. The tyrosine phosphatase STEP mediates AMPA receptor endocytosis after metabotropic glutamate receptor stimulation. J Neurosci. 2008; 28:10561–10566. [PubMed: 18923032]

Highlights

- Early life seizures (ELS) selectively enhance mGluR-mediated LTD (mLTD).
- ELS disrupt the localization of FMRP and PP2A. ELS also disrupts FMRP and S6K phosphorylation.
- ELS disrupt binding of S6K to the FMRP/PP2A/S6K complex; S6K is over-activated.
- mLTD is mediated by PP2A; this regulation is lost after ELS.
- ELS are associated with reduced socialization.

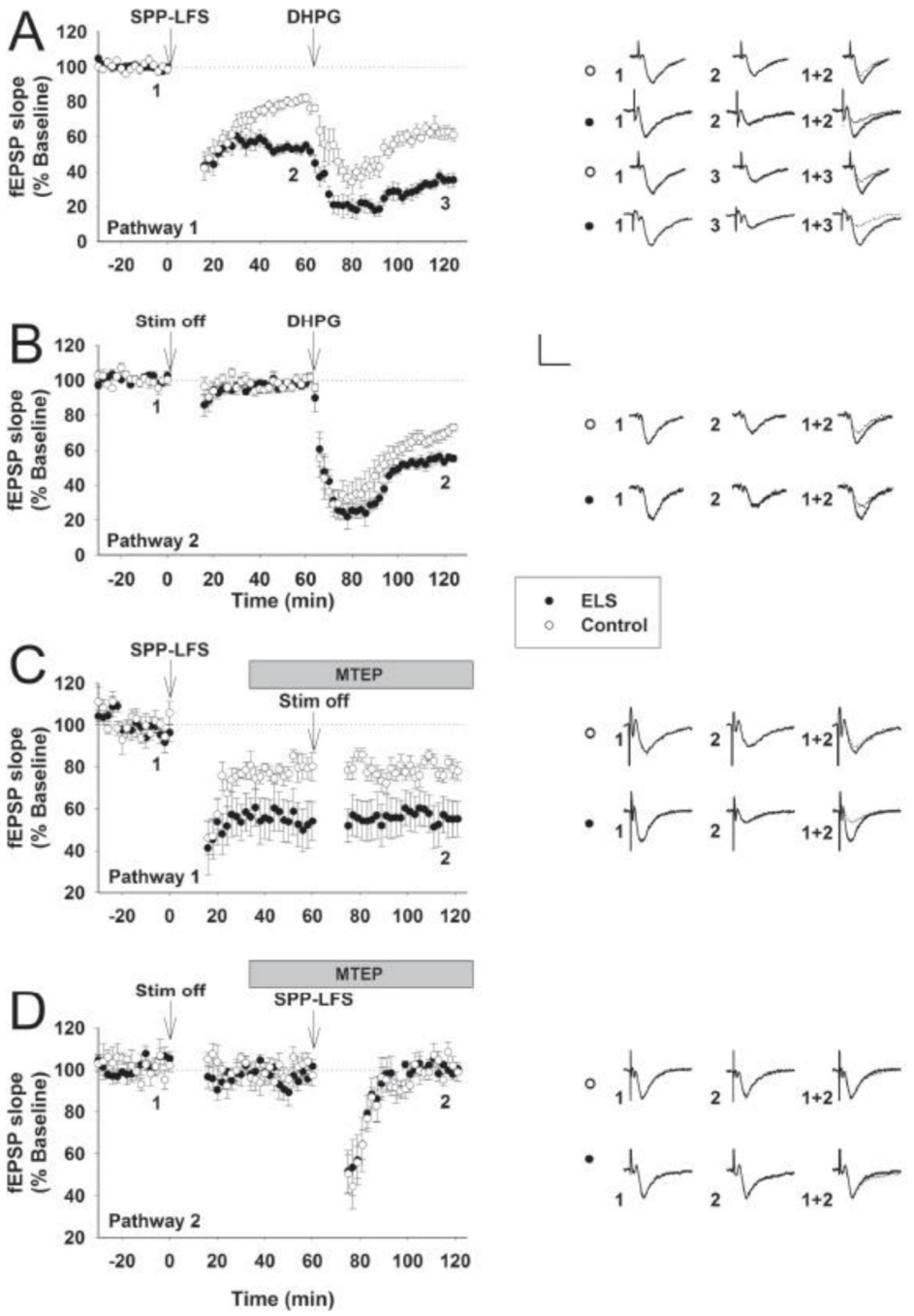

Figure 1. mLTD is preferentially enhanced following ELS at P60

In the presence of D-APV (50 μM), two-pathway protocol was used to investigate both stimulation-induced (A, SPP-LFS, Pathway 1) and chemical-induced (B, DHPG × 100 μM × 10 min, Pathway 2) mLTD for comparisons between ELS (filled circles) and control (open circles). fEPSP slopes, normalized to 100% baseline, are shown. Stimulation (ELS: 54.82± 2.52%, n = 12, control: 82.06± 2.55%, n = 8, $P < 0.001$, Student's t-test) and chemical mLTD (ELS: 55.12± 2.23%, n = 10, control: 72.874± 2.44%, n = 8, $P < 0.001$, Student's t-test) were significantly enhanced following ELS. In the presence of D-APV (50 μM), two-pathway protocol was used to investigate stimulation-induced mLTD induction in the absence of MTEP (C, Pathway 1; ELS: 57.65±9.73%, n=7, control: 85.41 ±2.43%, n=7,

P<0.013, Student's t-test) and in the presence of MTEP (500 nM) (D, Pathway 2; ELS: 98.282±3.01%, n=6, control: 98.92±4.24%, n=6, P=0.91, student's t-test). Insets show averages of 4 fEPSPs near the numerically indicated time points. Scale bar 0.5 mV × 15 msec.

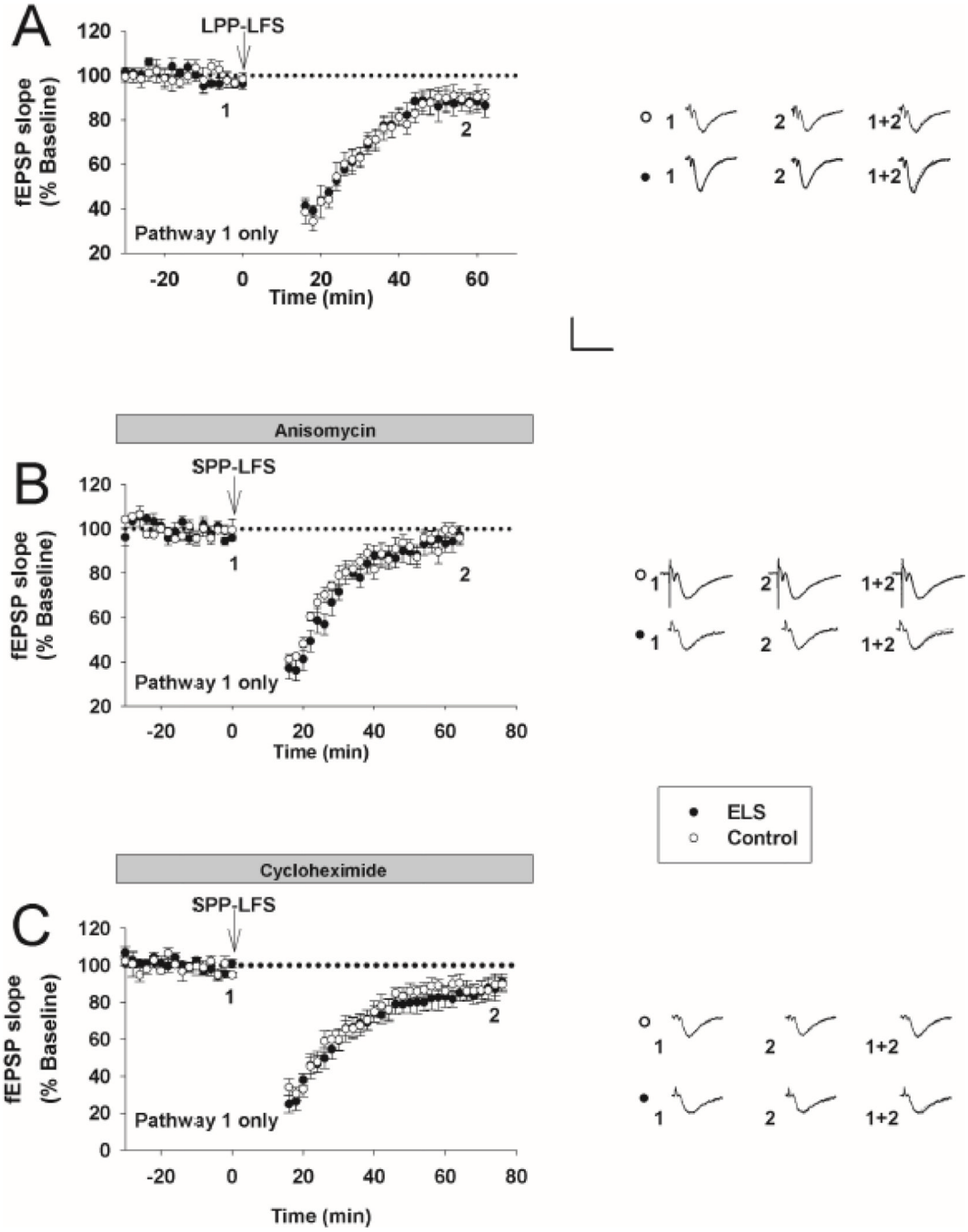

Figure 2. NMDAR-mediated LTD and protein synthesis is intact in mLTD following ELS at P60

A, Omitting D-APV with a different induction protocol (LPP-LFS), NMDAR-mediated LTD was not different (ELS: 88.82 ± 4.19%, n = 6, control: 89.58 ± 3.16%, n = 7, P = NS, Student's t-test). B, in the presence of anisomycin (20 μM), stimulus induced mLTD (SPP-LFS plus D-APV, 50 μM) was equally, and nearly totally, blocked following ELS (filled circles) compared to controls (open circles) (ELS: 94.22 ± 3.82%, n = 6, control: 98.05 ± 2.44%, n = 6, P = NS, Student's t-test). C, In the presence of cycloheximide (60 μM) stimulus induced mLTD (SPP-LFS plus D-APV, 50 μM) was equally, but not totally, blocked following ELS compared to controls (ELS: 91.02 ± 5.33%, n = 6, control: 89.58 ± 4.24%, n = 7, P = NS, Student's t-test). Insets show averages of 4 fEPSPs near the

numerically indicated time points. Scale bar 0.5 mV × 15 msec. fEPSP slopes, normalized to 100% baseline, are shown.

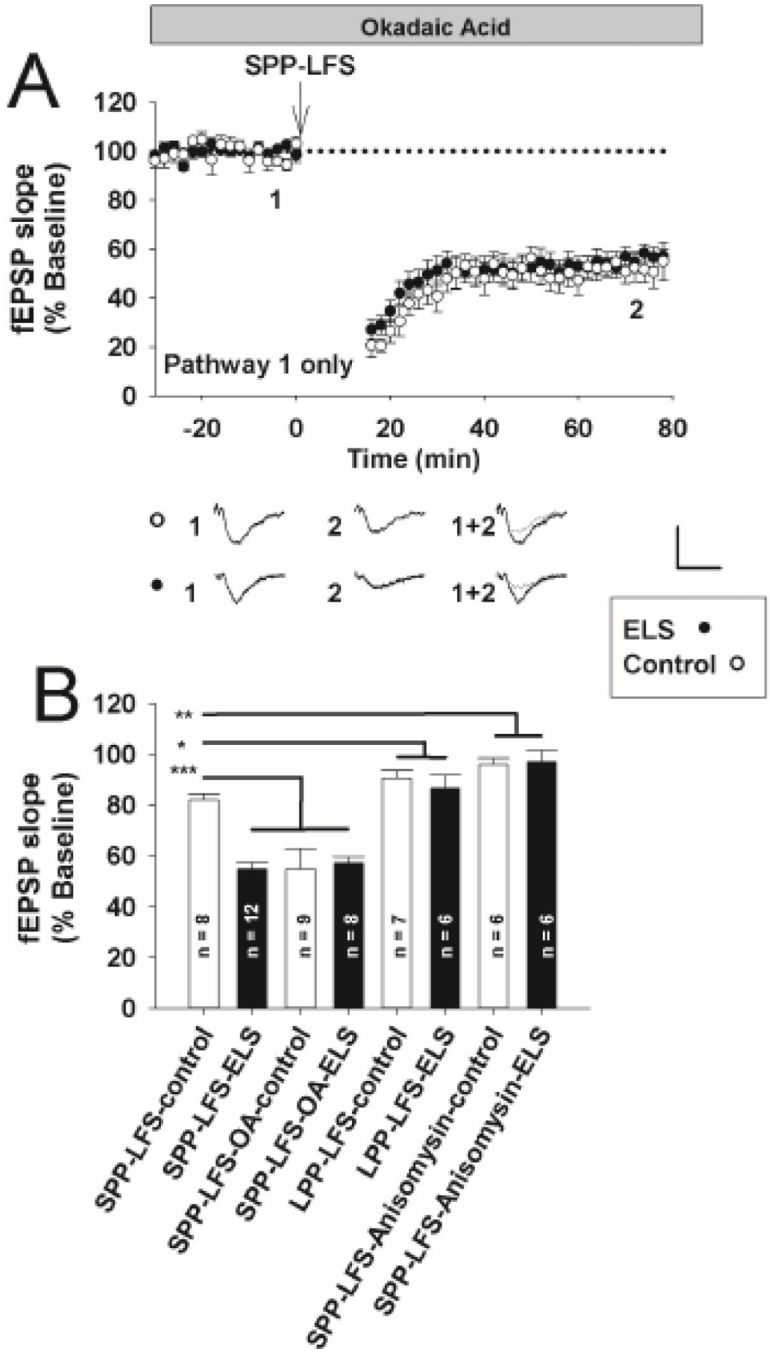

Figure 3. Blockade of PP2A–mediated exaggerated mLTD is occluded following ELS at P60

A, In the presence of okadaic acid (OA, 3 nM), stimulus induced mLTD (SPP-LFS plus D-APV, 50 μM) was similar in controls (open circles) compared to ELS (filled circles) (controls: 52.47 ± 4.49%, n = 8, ELS: 54.09 ± 4.99%, n = 9, P = NS, Student's t-test). Insets show averages of 4 fEPSPs near the numerically indicated time points. Scale bar 0.5 mV × 15 msec. fEPSP slopes, normalized to 100% baseline, are shown. B, Summary bar graph, ELS solid bars, control open bars. Significance of comparisons (ANOVA) is denoted by * = P<0.05, ** = P< 0.01, *** = P<0.001.

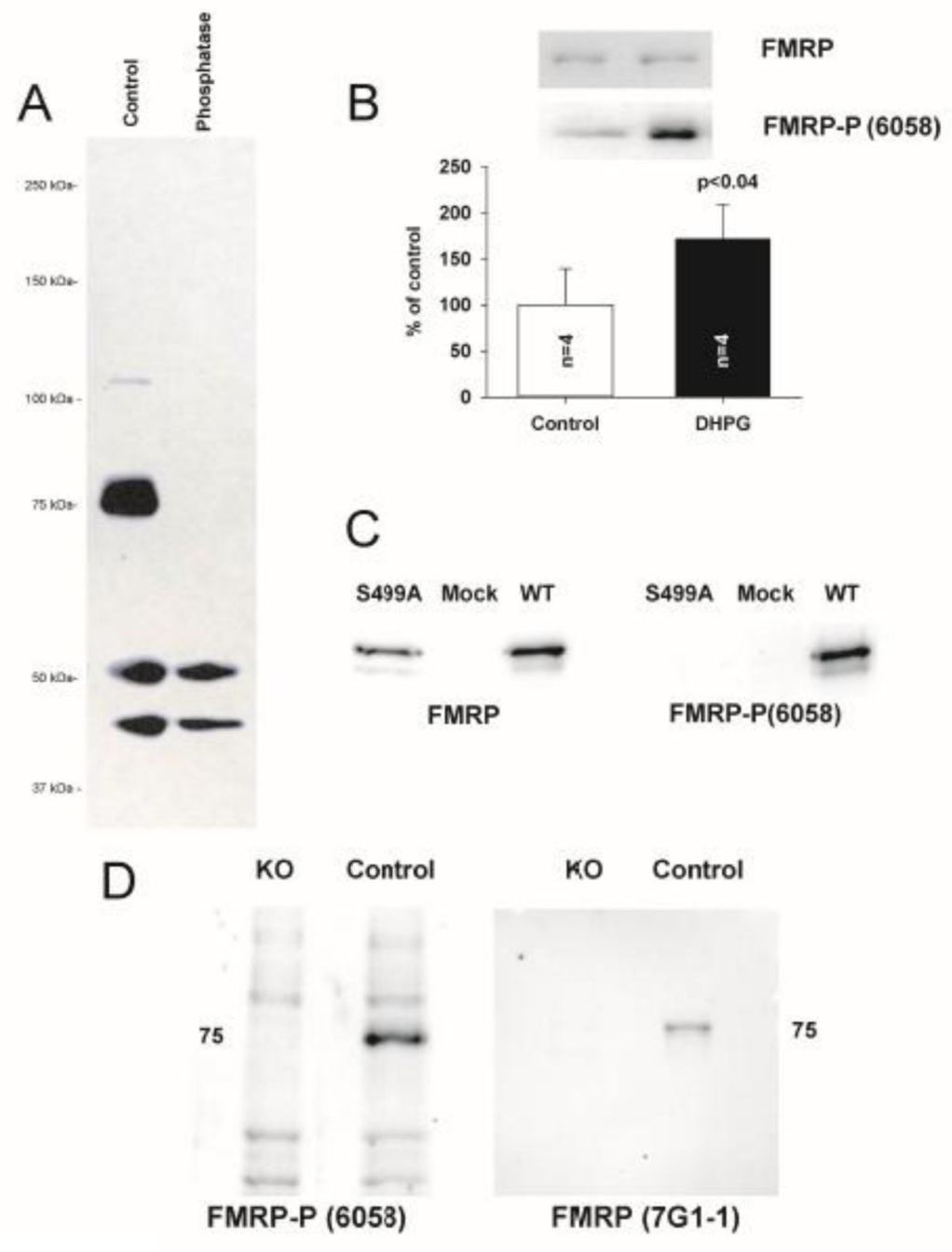

Figure 4. Characterization of phosphorylated FMRP antibody (6058)

A, In adult hippocampal slices, 6058 selectively labeled a band around 75kDa corresponding to the molecular weight of FMRP; intensity of this band was completely eliminated by phosphatase treatment, demonstrating that 6058 exclusively recognizes phosphoprotein. B, Adult hippocampal slices treated with DHPG (100 μM × 30 mins) were compared to untreated matched-slice controls. Intensity of 6058 immunoreactivity at 75 kDa was increased by DHPG treatment, demonstrating that 6058 exclusively recognizes relevant biologically active FMRP phosphoprotein. Quantification of DHPG-induced phosphorylation of FMRP (control 6058::total ratio: 100±39.12, n = 4, treated 6058::total ratio: 171.21±37.47, n = 4, p< 0.04, Repeated Measures ANOVA). C, 6058

immunoreactivity is absent in HEK293 cells transfected with S499A–FMRP mutant, while present when transfected with wild-type FMRP. D, FMR1 KO mice do not display immunoreactivity at 75 kDa when probed with antibody 6058 compared to controls which display robust immunoreactivity.

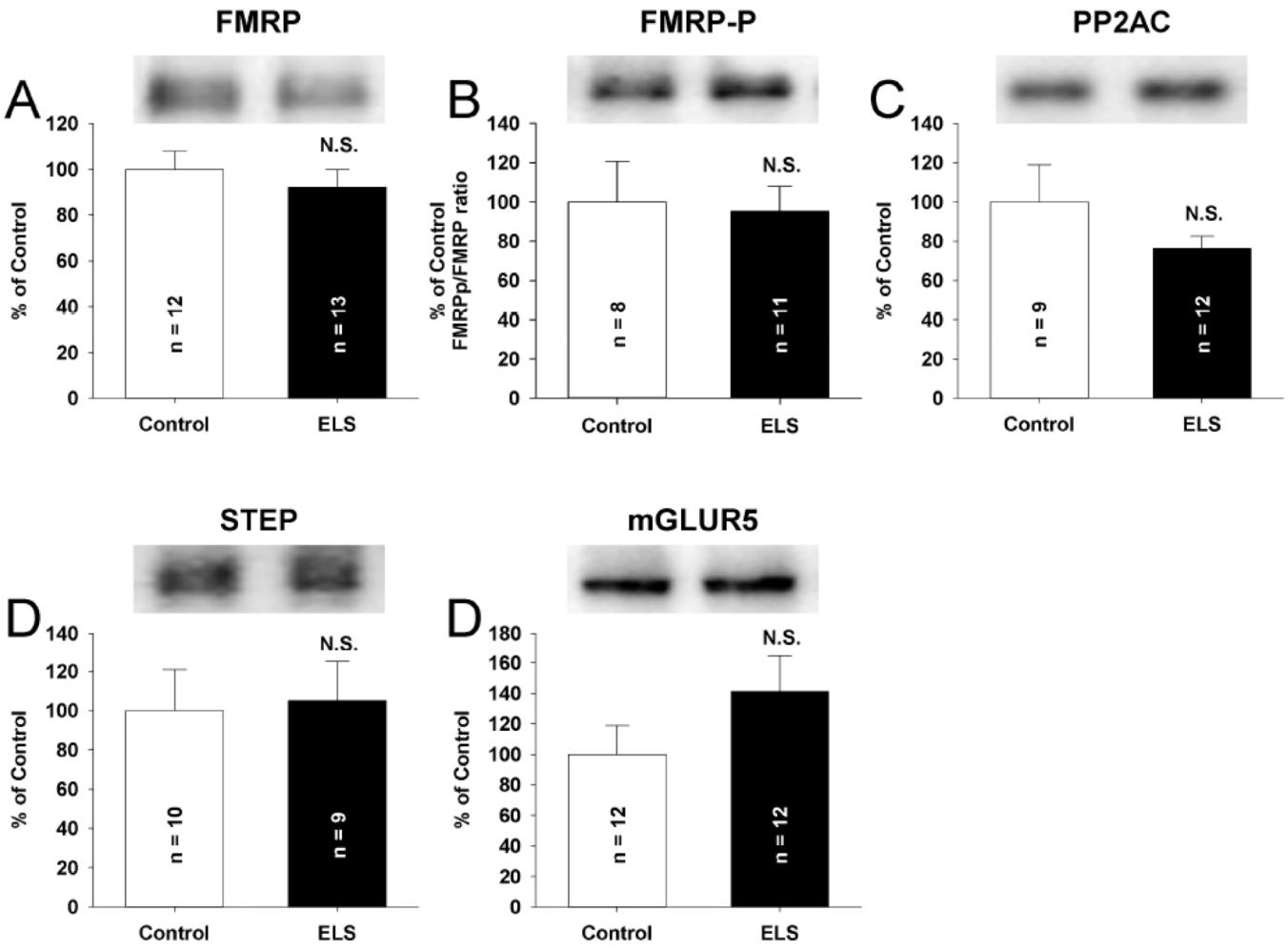

Figure 5. Total expression of mLTD linked proteins is unchanged following ELS at P60

No alterations in the total expression of FMRP (A) (ELS: 92.05 ± 7.95%, n = 13, control: 100± 7.95%, n = 12, P = NS, Student's t-tests), FMRP-P (B) (ELS: 95.27 ± 12.64%, n = 11, control: 100± 20.81%, n = 8, P = NS, Student's t-tests), the core, catalytic subunit of PP2A (PP2AC) (C) (ELS: 76.26 ± 6.32%, n = 12, control: 100 ± 19.13%, n = 9, P = NS, Student's t-tests), STEP (D) (ELS: 105.11 ± 20.00%, n = 9, control: 100 ± 21.06%, n = 10, P = NS, Student's t-tests) or mGluR5 (E) (ELS: 141.12 ± 23.36%, n = 12, control: 100 ± 18.88%, n = 12, P = NS, Student's t-tests), were observed. Semi-quantitative western-blot technique(Cornejo et al., 2007) was used to determine immunoreactivity/mg loaded protein, which were normalized to controls (see Methods). Typical blots with equivalent protein loading shown. Solid bars ELS, open bars control.

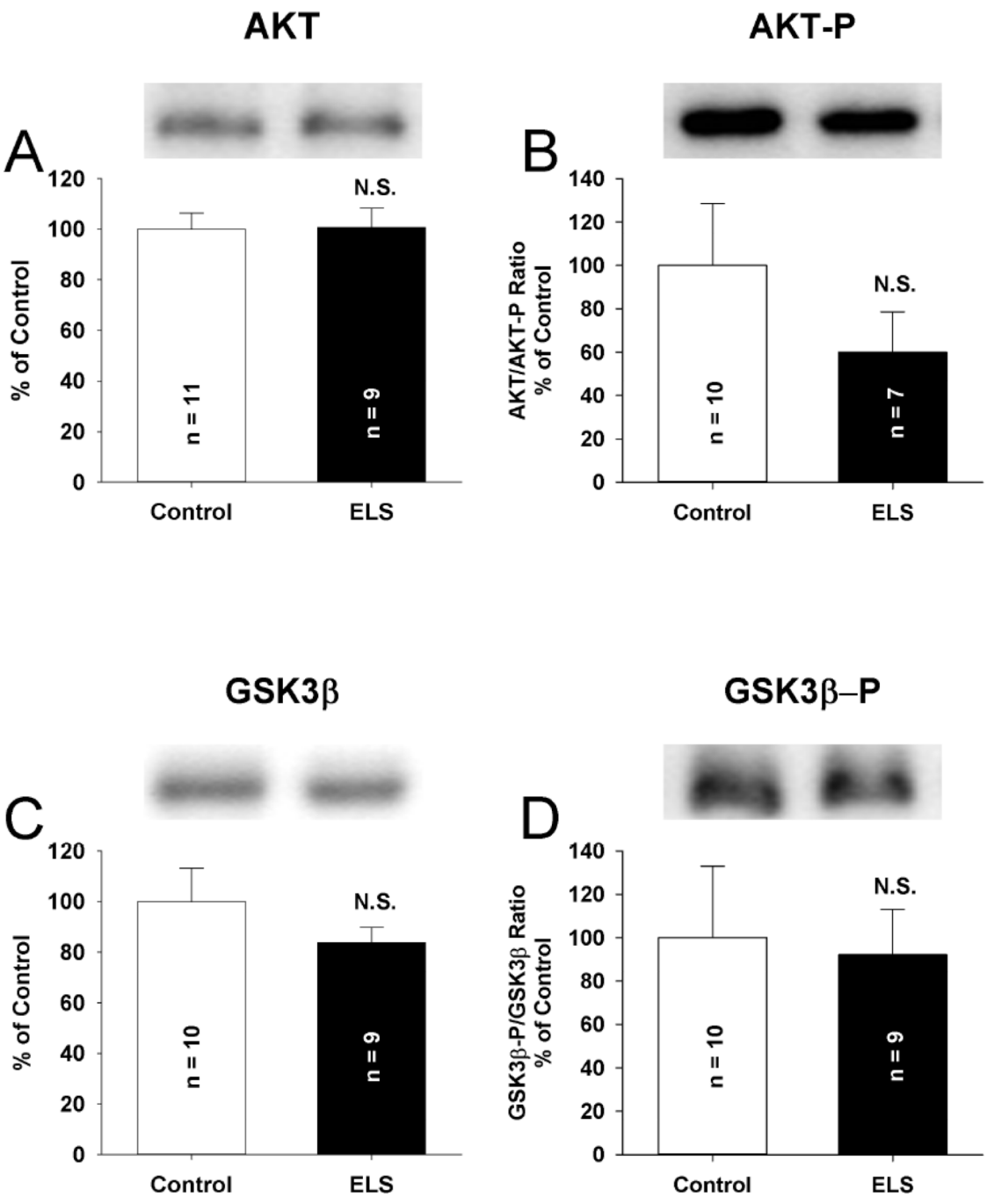

Figure 6. Total expression of LTD linked kinases is unchanged following ELS at P60

No alterations were observed in the total expression of AKT (A) (ELS: 100.63 ± 7.72%, n = 9, control: 100.00 ± 6.48%, n = 11, P = NS, Student's t-tests) or phosphorylated Akt (Ser 473) (B) (ELS: 60.07 ± 18.5%, n = 7 control: 100 ± 28.51%, n = 10, P = NS, Student's t-tests) following ELS compared to controls. No alterations were observed in the total expression of GSK3β (C) (ELS: 83.70 ± 6.09%, n = 9, control: 100.00 ± 13.15%, n = 10, P = NS, Student's t-tests) or phosphorylated GSK3β (Ser 9) (D) (ELS: 92.21 ± 20.72%, n = 9, control: 100.00 ± 32.93%, n = 10, P = NS, Student's t-tests) following ELS compared to controls. Semi-quantitative western-blot technique(Cornejo et al., 2007) was used to determine immunoreactivity/mg loaded protein, which were normalized to controls (see

Methods). Typical blots with equivalent protein loading shown. Solid bars ELS, open bars control.

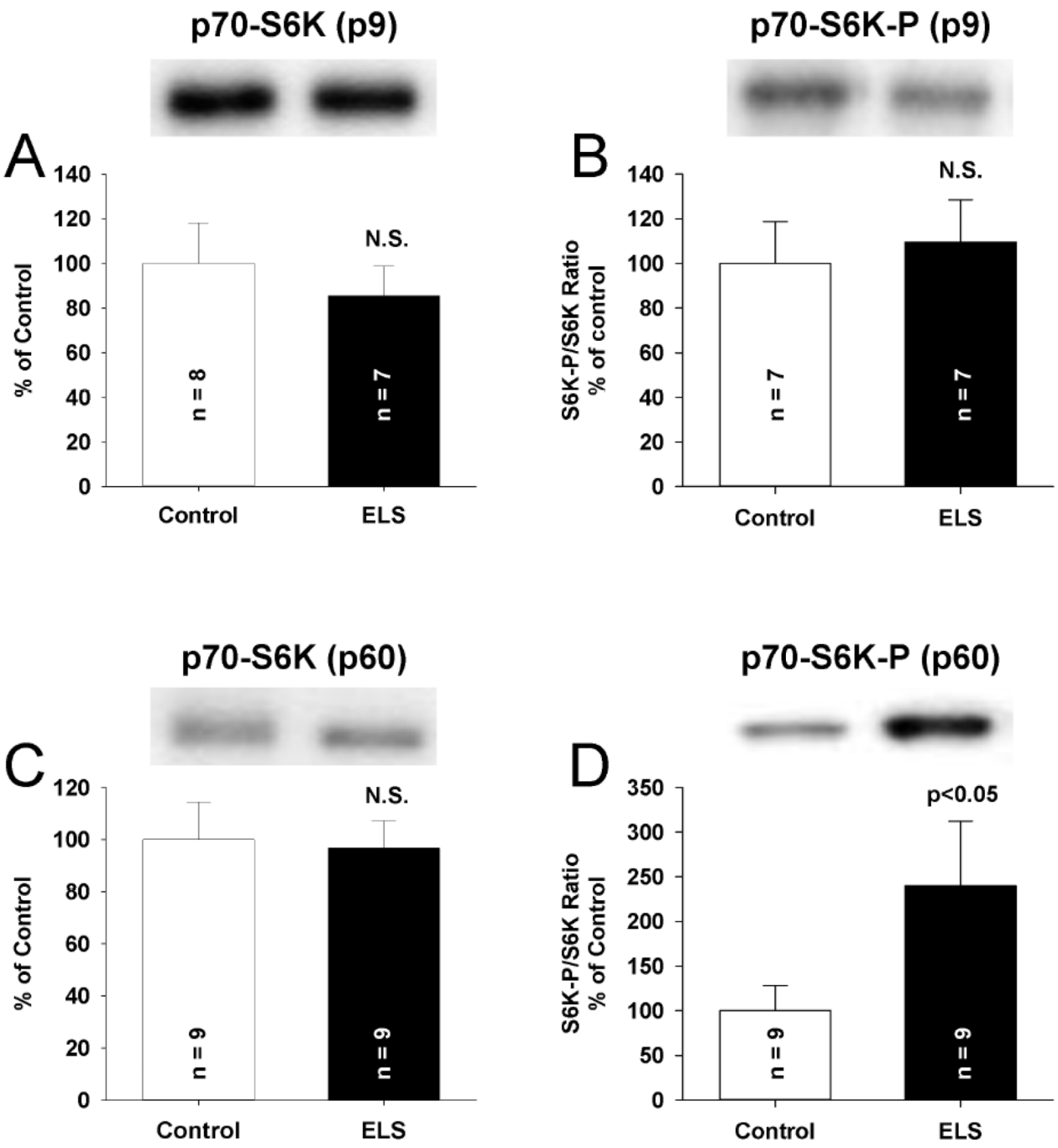

Figure 7. Increased S6K phosphorylation only chronically following ELS

A, No alteration of total S6K (ELS: 85.60 ± 13.11%, n = 8, control: 100.00 ± 18.07%, n =7, P = NS, Student's t-tests) was found 2 days following ELS (P9) compared to control. B, No alteration of phosphorylated S6K (Thr 389) (ELS: 109.66 ± 18.90%, n = 7, control: 100.00 ± 18.76%, n =7, P = NS, Student's t-tests) was found 2 days following ELS (P9) compared to control. C, No alteration of total S6K (ELS: 96.70 ± 10.51%, n = 9, control: 100.00 ± 14.41%, n =9, P = NS, Student's t-tests) was found weeks (P60+) following ELS compared to control. D, ELS increased phosphorylated S6K (Thr 389) (ELS: 239.51 ± 72.35%, n = 9, control: 100.00 ± 28.15%, n = 9, P < 0.05, Student' s t-test) weeks (P60+) following ELS compared to control. Semi-quantitative western-blot technique(Cornejo et al., 2007) was

used to determine immunoreactivity/mg loaded protein, which were normalized to controls (see Methods). Typical blots with equivalent protein loading shown. Solid bars ELS, open bars control.

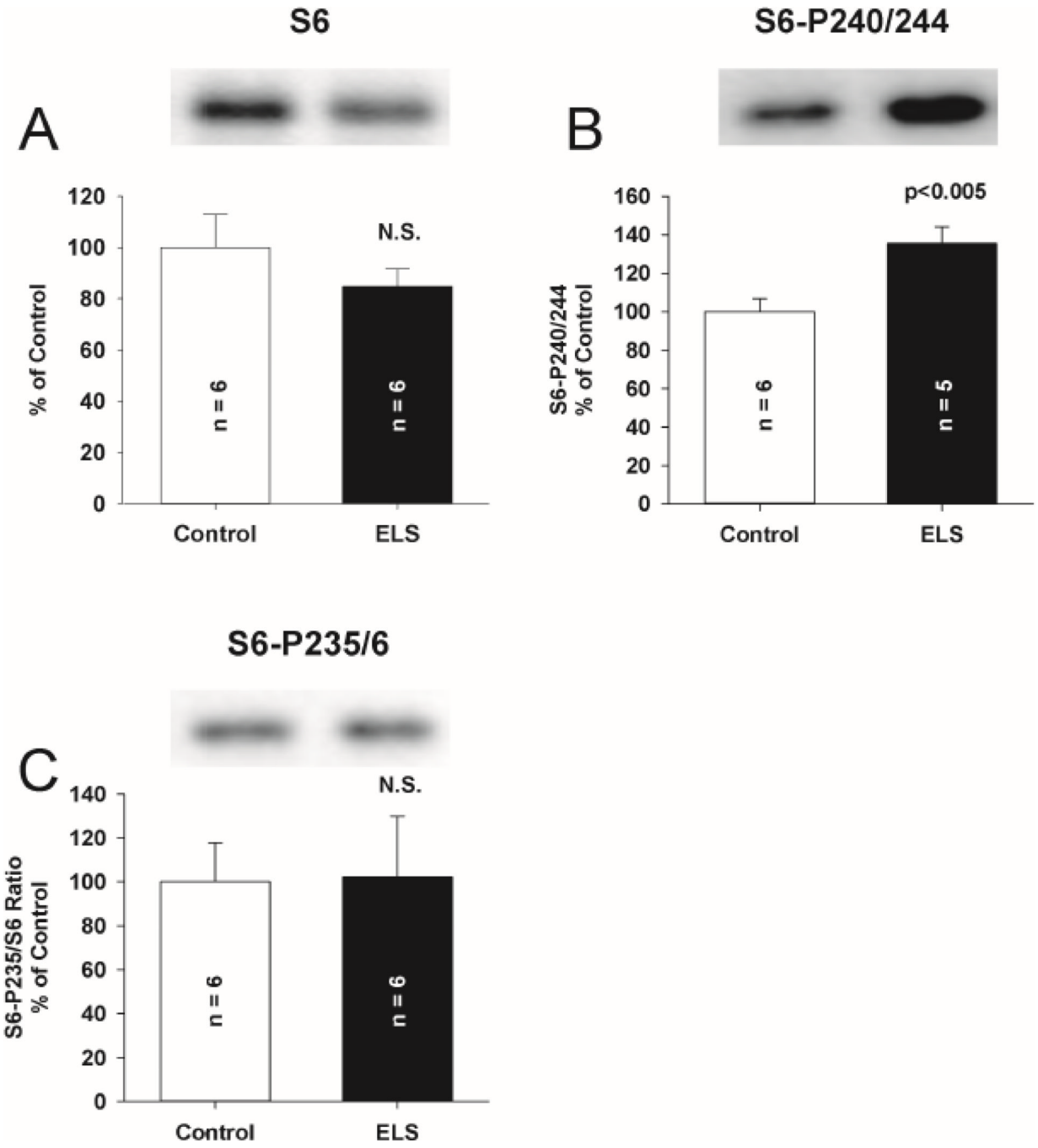

Figure 8. Expression of translational kinase S6 and selected phosphorylated isoforms following ELS at P60

A, Total expression of S6 was not affected by ELS compared to control (ELS: 84.78 ± 6.74%, n = 6, control: 100.00 ± 12.83%, n = 6, NS, Student's t-tests). Expression of phosphorylated S6 isoform (B), Ser 240/244 was significantly elevated by ELS (ELS: 135.32 ± 8.81%, n = 5, control: 100.00 ± 6.69%, n = 6, P <0.005, Student's t-tests). Expression of phosphorylated isoform Ser 235/236 (C) was not altered by ELS (ELS: 102.3 ± 27.48%, n = 6, control: 100.00 ± 17.84%, n = 6, P = NS, Student's t-tests). Semi-quantitative western-blot technique(Cornejo et al., 2007) was used to determine

immunoreactivity/mg loaded protein, which were normalized to controls (see Methods). Typical blots with equivalent protein loading shown. Solid bars ELS, open bars control.

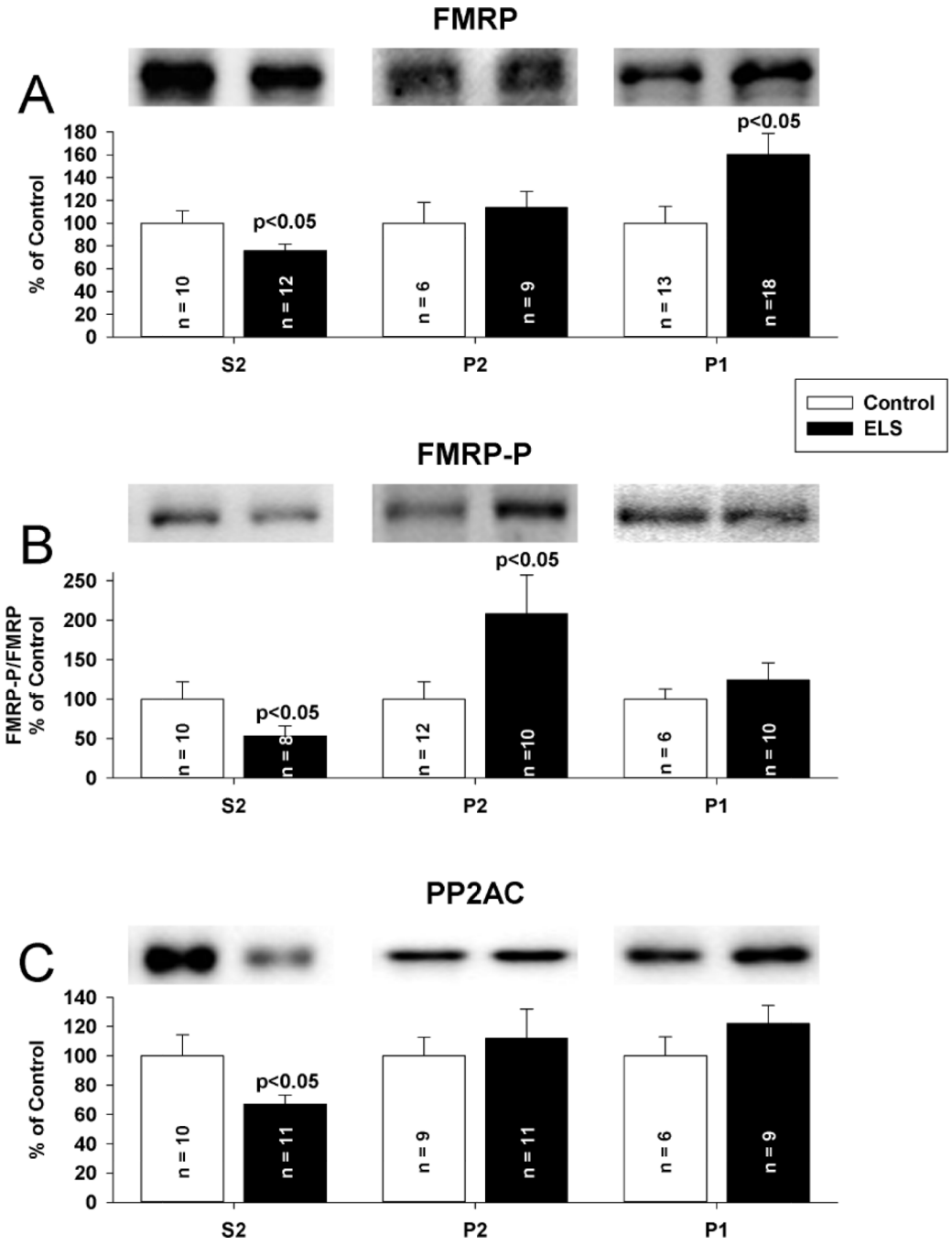

Figure 9. Selective compartmental alterations of FMRP and PP2AC following ELS at P60

Subcellular fractionation reports a concentration of each protein in a given fraction; concentrations for each protein were normalized to control for that fraction. A, FMRP was removed from the cytosolic compartment (S2 fraction, ELS: 75.87 ± 5.66%, n = 12; control: 100 ± 10.67%, n = 10, P < 0.05, Student's t-test). FMRP P2 (synaptosomal) fraction was not changed (ELS: 113.40 ± 14.39%, n = 9, control: 100 ± 16.12%, n = 6, P = NS, Student's t-test). FMRP P1 (nuclear) fraction was significantly increased following ELS (ELS: 160.11 ± 18.60%, n = 18, control: 100.00 ± 14.69, n = 13, P < 0.05, Student's T-test). B, FMRP-P was reduced in the cytosolic compartment (S2 fraction) following ELS (ELS: 53.14 ± 12.78, n = 8; control: 100 ± 21.98, n = 10, P < 0.05, Students's t-test). Following ELS, FMRP-P

was increased in the synaptosomal fraction (P2)(ELS: 208.13 ± 49.40, n = 10; ; control: 100 ± 22.01, n = 12, $P < 0.05$). FMRP-P was unchanged in the P1 (nuclear) fraction (ELS: 123.81 ± 22.15, n = 10, control: 100.00 ± 12.61, n = 6, P = NS). C, PP2AC was removed from the cytosolic compartment (S2 fraction, ELS: 66.88 ± 6.30%, n = 11 control: 100 ± 14.32%, n = 10, $P < 0.05$, Student's t-test). PP2AC P2 (synaptosomal) fraction was not changed (ELS: 111.83 ± 20.23%, n = 11, control: 100 ± 12.64%, n = 9, P = NS, Student's t-tests). The PP2AC P1 (nuclear) fraction was not changed following ELS (ELS: 122.11 ± 12.30, n = 9, control: 100.00 ± 12.97, n = 6, P = NS). Purity of fractions was determined by restriction of PSD-95 to the P2 fraction (supplementary Figure 4). Semi-quantitative western-blot technique(Cornejo et al., 2007) was used to determine immunoreactivity/mg loaded protein, which were normalized to controls. Typical blots with equivalent protein loading shown. Solid bars ELS, open bars control.

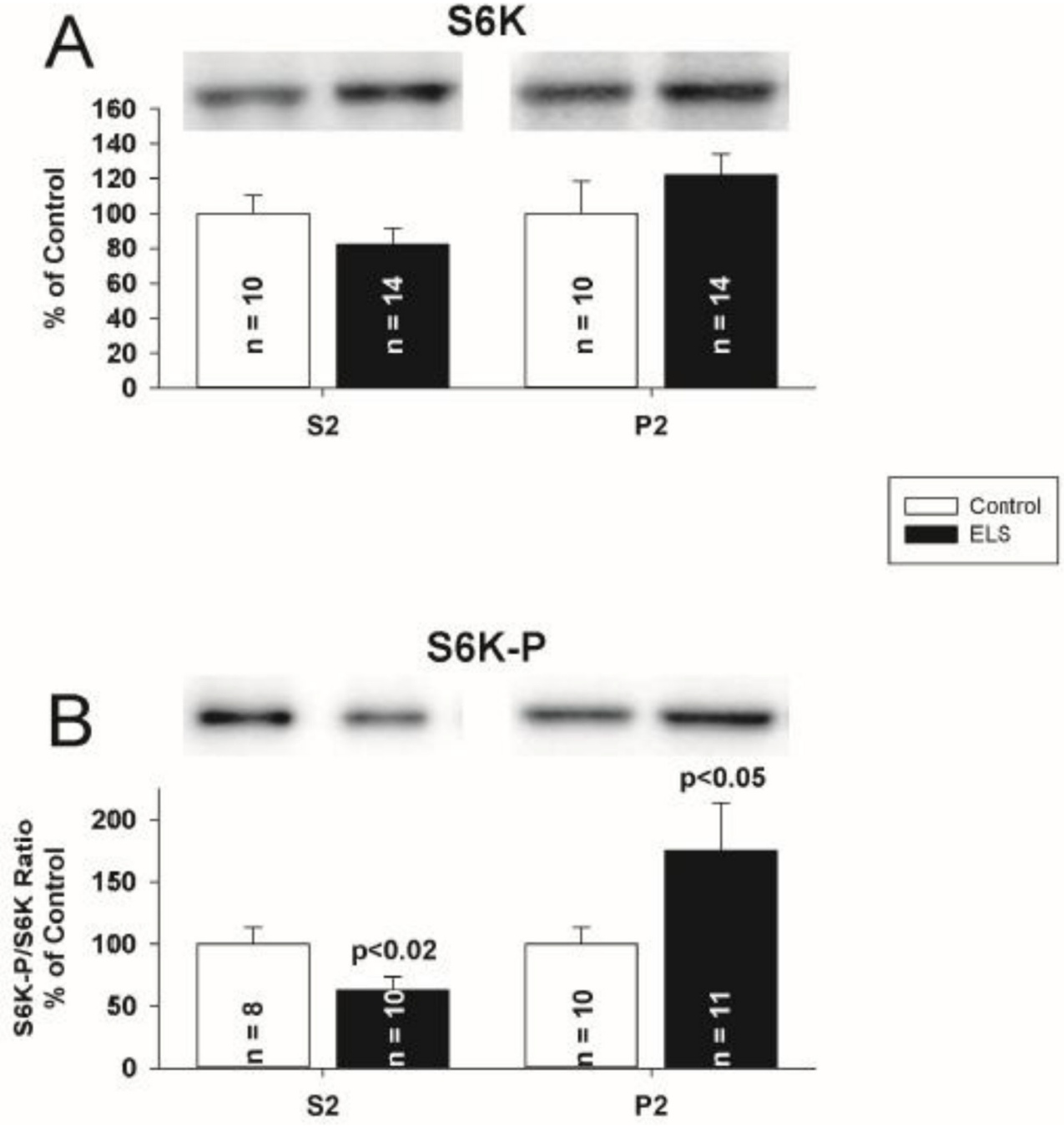

Figure 10. ELS does not mediate alterations in localization of S6K, but does mediate changes in S6K–P at P60

A, S6K was not significantly removed from the cytosolic compartment, though a trend similar to PP2A and FRMP was suggested (S2 fraction, ELS: 82.01 ± 9.45%, n = 14; control: 100 ± 10.50%, n = 10, P = NS, Student's t-test). S6K P2 (synaptosomal) fraction was not changed (ELS: 121.90 ± 12.18%, n = 14, control: 100 ± 18.58%, n = 10, P = NS, Student's t-tests). B, Phosphorylated S6K (Thr 389) was significantly reduced in the cytosolic compartment (S2 fraction, ELS: 63.13 ± 10.35%, n = 10; control: 100 ± 13.16%, n = 8, P < 0.02, Student's t-test). Phosphorylated S6K (Thr 389) was significantly increased in the P2 (synaptosomal) fraction (ELS: 175.00 ± 38.58%, n = 11, control: 100 ± 13.04%, n =

10, $P < 0.05$, Student's t-tests). Semi-quantitative western-blot technique(Cornejo et al., 2007) was used to determine immunoreactivity/mg loaded protein, which were normalized to controls (see Methods). Typical blots with equivalent protein loading shown. Solid bars ELS, open bars control.

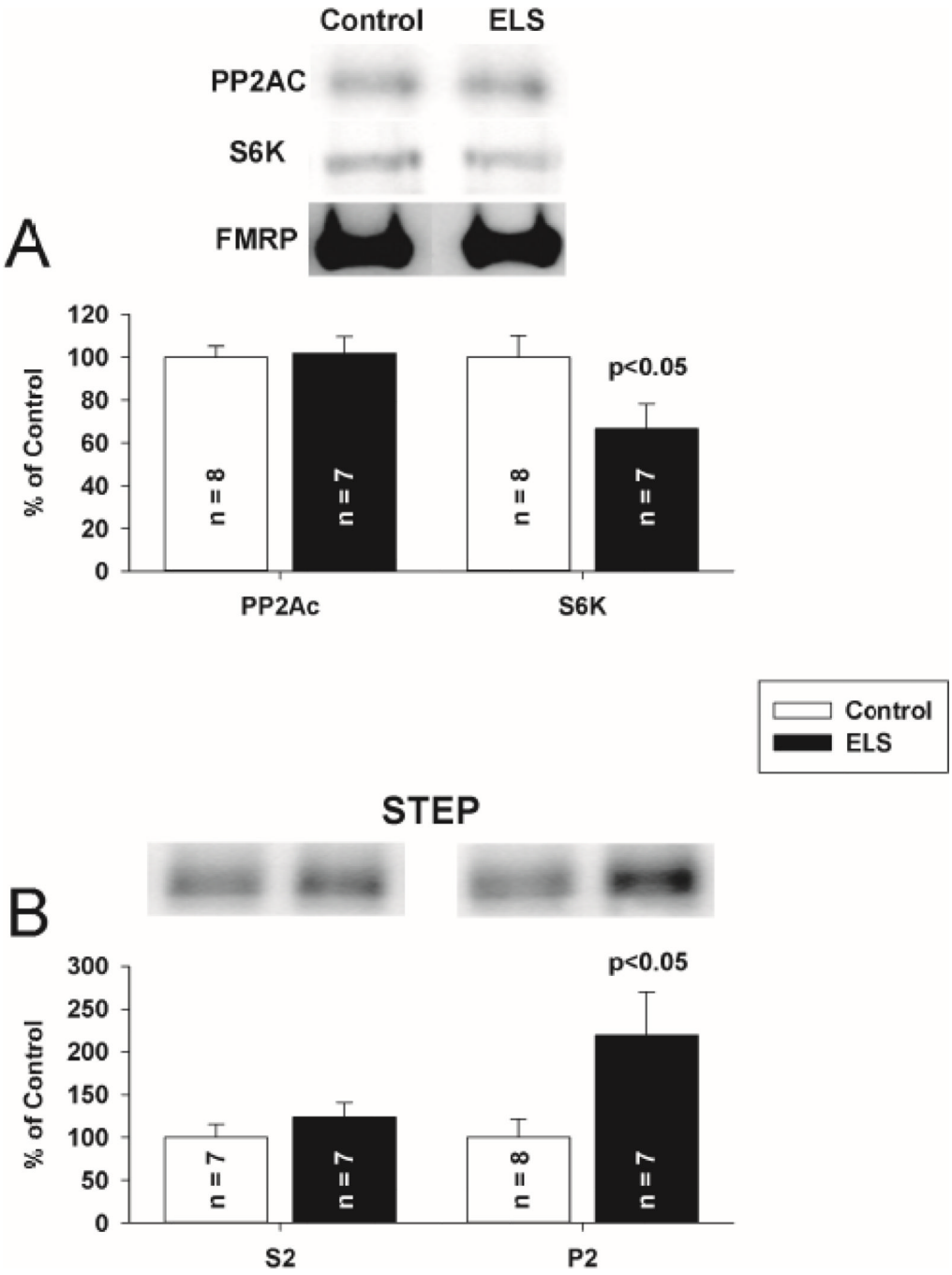

Figure 11. ELS mediates loss of S6K from FMRP-PP2A–S6K complex and a decrease in synaptosomal STEP at P60

A, FMRP-IPs from CA1 hippocampal lysates probed for PP2AC (ELS: 101.77 ± 7.93%, n = 7; control: 100 ± 5.17%, n = 8, P = NS, Student's t-test) and S6K (ELS: 65.52 ± 11.63%, n = 7; control: 100 ± 10.22%, n = 8, P < 0.05, Student's t-test) show unchanged interaction of FMRP and PP2AC but reduced interaction of FMRP and S6K associated with ELS. B, STEP S2 (cytosolic) fraction was not changed (ELS: 123.40 ± 17.70%, n = 7, control: 100 ± 15.51%, n = 7, P = NS, Student's t-tests). STEP was increased in the synaptosomal compartment (P2 fraction, ELS: 218.95 ± 51.05%, n = 7; control: 100 ± 21.16%, n = 8, P < 0.05, Student's t-test). Solid bars ELS, open bars control.

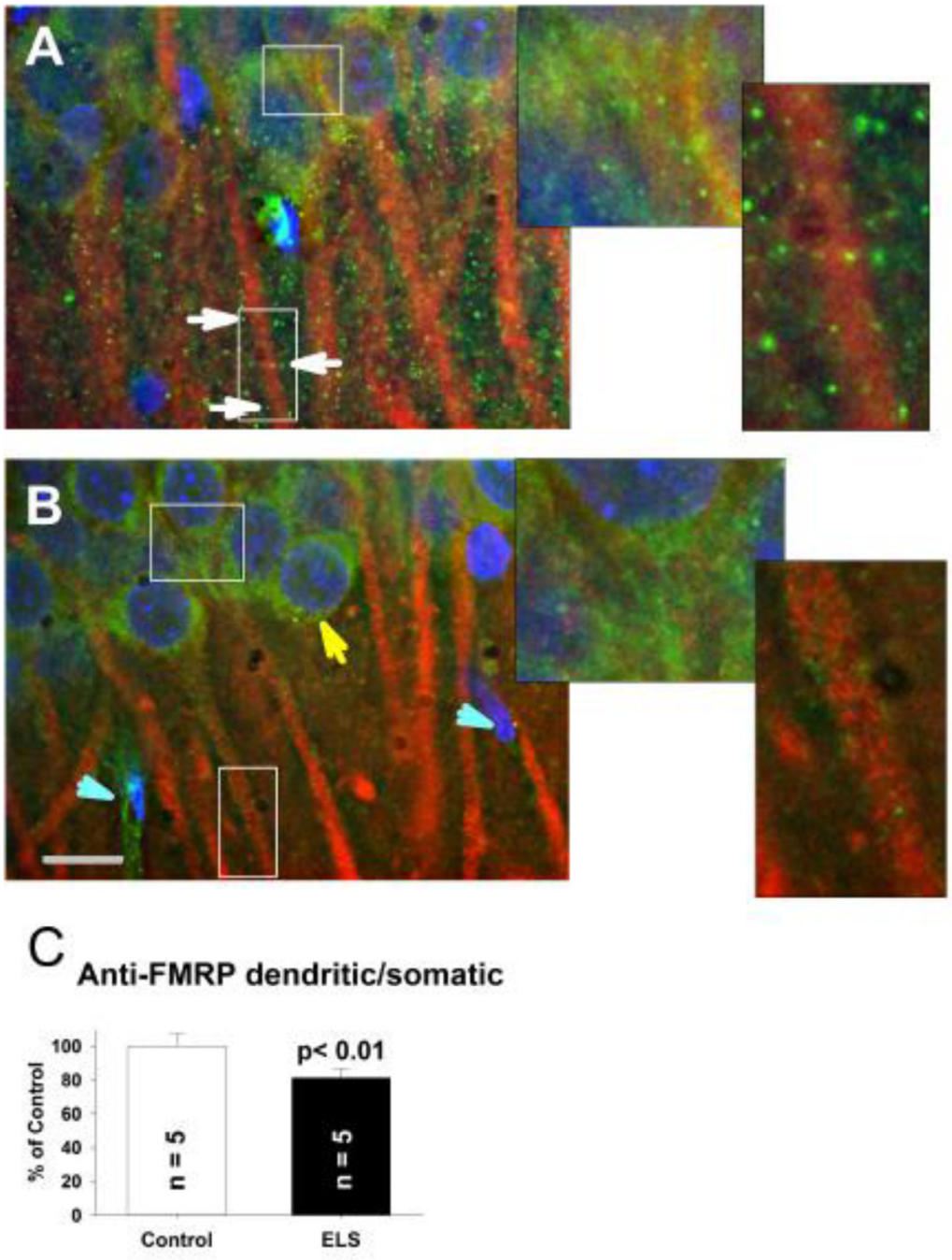

Figure 12. FMRP localization after ELS

A, At P60+, anti-FMRP staining (green) in controls forms puncta (white arrows) presumably near synapses(Antar et al., 2005) along anti-MAP2 stained (red) dendrites in CA1 region of the hippocampus, with light peri-nuclear staining. Enlarged insets from respective somatic and dendritic regions are shown. B, Following ELS, at P60+ FMRP positive puncta are nearly completely lost along dendrites with relative perinuclear accumulation (yellow arrow). Nuclei are counterstained with DAPI (blue) to show the location of principal neurons in stratum pyramidale and assist with differentiating non-neuronal elements (turquoise arrowheads). Scale bar 10 μm. Enlarged insets from respective somatic and dendritic regions are shown. Images shown in A and B were captured at a similar slice

depth. C, Quantification of FMRP translocation from dendritic to somatic regions. The ratio of dendritic to somatic anti-FMRP fluorescence intensity (normalized by the ratio of anti-MAP2 fluorescence intensity to control for subtle differences in neuronal densities and obtained through all *x*–*y* planes in the *z*-stack) was significantly less (0.495 ± 0.027, N = 5) following ELS compared to controls (0.624 ± 0.0423, N = 5, P < 0.01, repeated measures ANOVA). The ratio of anti-MAP2 fluorescent intensities was not significantly different between ELS and controls, indicating no change in neuronal density. Solid bar ELS, open bar control.

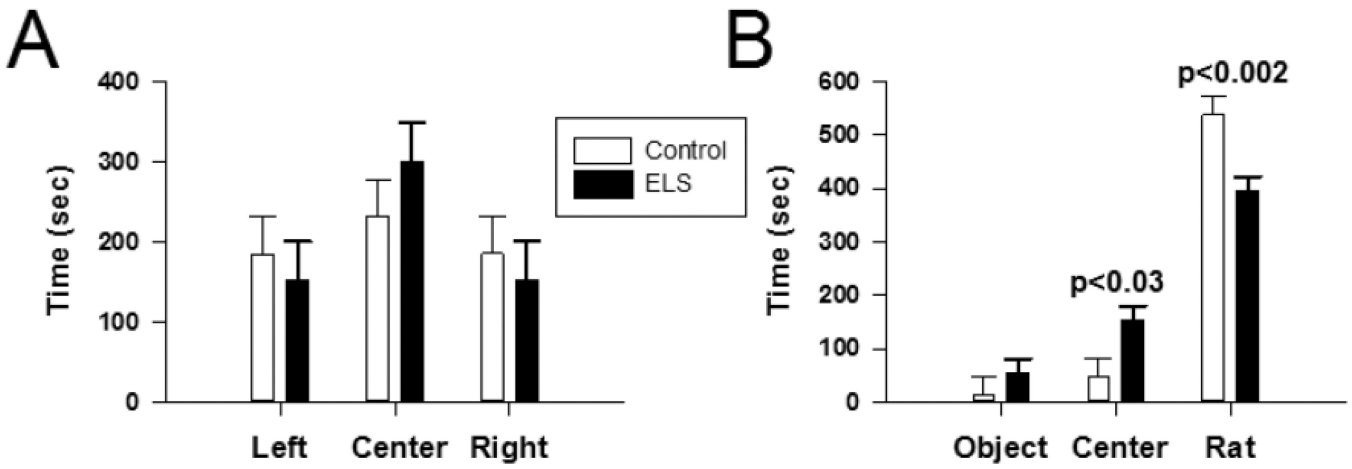

Figure 13. Abnormal socialization following ELS at P60

A, In trial #2 (conducted with an empty apparatus, i.e. no novel object or novel rat), neither control or ELS animals displayed a significant preference for any of the three chambers (P=0.48, two way ANOVA). B,During trial #3, both ELS and control animals spent significantly more time with the novel rat (ELS time with novel rats: 393.80 ± 40.66, ELS time with novel object: 53.60 ± 16.64, $P < 0.05$; control time with novel rat: 537.86 ± 18.54, control time with novel object: 13.29 ± 8.823, $P < 0.05$). However, ELS animals spent significantly less time in the novel rat chamber compared to controls (control: 537.86±33.40 s, n=9, ELS:393.80±27.95 s, n=11, P=0.002, two way ANOVA). Solid bar ELS, open bar control.

Table 1

Primary antibodies used for western-blot analysis; (o/n) = overnight, IP = immunoprecipitation.

Primary antibody	Size (kDa)	Diluent	Host name	Dilution factor	Company
AKT P (Ser473)	60	1%BSA	rabbit	1/500	Cell Signaling
AKT	60	1%milk	mouse	1/1000	Cell Signaling
FLAG		1% milk	mouse	1/1000	Sigma
FMRP 1C3	75	1%milk	mouse	1/500	Millipore
FMRP 7G1–1	75	IP	mouse	IP	DSHB
Phospho-FMRP 6058	75	1%milk	rabbit	1/1000	PhosphoSolutions
GSK3B P (Ser9)	46	1%milk	rabbit	1/500	Cell Signaling
GSK3B	46	1%milk	rabbit	1/500	Cell Signaling
mGLUR 5	132	1%milk	rabbit	1/300	Millipore
PP2A C subunit	36,38	1%milk	rabbit	1/1000	Cell Signaling
S6	32	5%BSA	rabbit	1/1000	Cell Signaling
S6 P (Ser235/236)	32	5%BSA	rabbit	1/1000 (o/n)*	Cell Signaling
S6 P (Ser240/244)	32	5%BSA	rabbit	1/1000	Cell Signaling
STEP	61	1%BSA	mouse	1/1000	Cell Signaling
p70-S6 Kinase	70	5%BSA	rabbit	1/500 (o/n)*	Cell Signaling
p70-S6 Kinase P (Thr389)	70	5%BSA	rabbit	1/500	Cell Signaling